CDOT-CSM-R-93-20

ANALYTICAL SIMULATION OF ROCKFALL PREVENTION FENCE STRUCTURES

by

G.G.W. Mustoe and H.P. Huttelmaier
Department of Engineering
Colorado School of Mines

April 1993

Prepared under contract with the
Colorado Department of Transportation
in cooperation with the U.S. Department
of Transportation, Federal Highway
Administration

Technical Report Documentation Page

1. Report No.	2. Government Accession No.	3. Recipient's Catalog No.
CDOT-CSM-R-93-20		

4. Title and Subtitle	5. Report Date
Analytical Simulation of Rockfall Prevention Fence Structures	April 1993
	6. Performing Organization Code

7. Author(s)	8. Performing Organization Rpt.No.
G.G.W. Mustoe and H.P. Huttelmaier	CDOT-CSM-R-93-20

9. Performing Organization Name and Address	10. Work Unit No. (TRAIS)
Colorado School of Mines Department of Engineering Golden, Colorado 80401	11. Contract or Grant No.

12. Sponsoring Agency Name and Address	13. Type of Rpt. and Period Covered
Colorado Department of Transportation 4201 East Arkansas Avenue Denver, Colorado 80222	Final Report
	14. Sponsoring Agency Code

15. Supplementary Notes

Prepared in Cooperation with the U.S. Department of Transportation Federal Highway Administration

16. Abstract

This report describes the research work performed for the Colorado Department of Transportation (CDOT) during the period from June 1991 to March 1993, under the CSM Contract No. 3422.

The work performed during this contract included the following tasks: (i) the development of a novel numerical model for the dynamic simulation of a rockfall prevention fence using the discrete element method (DEM), (ii) the numerical implementation of the DEM numerical model in a computer code to be used by engineers at CDOT, and (iii) demonstration and validation of the DEM computer technique to simulate rockfall impacts against rockfall fences.

The original DEM numerical model was designed to analyze flexible rockfall prevention fences that were comprised of a single layer of columnar attenuators. In an additional research task funded under this contract the DEM model was extended to deal with fences with two layers of attenuators.

17. Key Words	18. Distribution Statement
Rockfall Prevention Rockfall Structures Discrete Element Method	No Restrictions: This report is available to the public through the National Technical Info. Service. Springfield, VA 22161

19.Security Classif. (report)	20.Security Classif. (page)	21. No. of Pages	22. Price
Unclassified	Unclassified	79	

TABLE OF CONTENTS

SUMMARY

This report describes the research work performed for the Colorado Department of Highways during the period from June 1991 to March 1993, under the research contract entitled ***Analytical Simulation of Rockfall Prevention Fence Structures***, CSM Contract No. 3422.

The work performed during this contract included the following tasks:(i) the development of a novel numerical model for the dynamic simulation of a rockfall prevention fence using the discrete element method (DEM), (ii) the numerical implementation of the DEM numerical model in a computer code to be used by engineers at the Colorado Department of Highways, and (iii) demonstration and validation of the DEM computer technique to simulate rockfall impacts against rockfall fences.

The original DEM numerical model was designed to analyze flexible rockfall prevention fences that were comprised of a single layer of columnar attenautors. In an additional research task funded under this contract the DEM model was extended to deal with fences with two layers of attenuators. The details of this additional research work are contained in Appendix I.

The dynamics simulation software was developed on an Intel based CPU 80486 microcomputer. This hardware environment was also used to perform the dynamic analyses which are described herein.

1.0 INTRODUCTION

The purpose of a rockfall prevention fence is to decrease the kinetic energy of a falling rock or rocks down a mountain valley. Such fences are installed near mountain highways to minimize the risk of automobile accidents caused by rockfall events. The fence type being investigated consists of hanging columnar attenuator masses assembled of used truck tires and rims, threaded onto a steel rod, which are suspended from a horizontal overhead wire cable and connected by a bottom cable (see Fig. 1). When a rock hits the fence the hanging columns begin to move in a pendulum-like motion. This mechanism transfers a significant amount of the rock's kinetic energy during the impact phase. Since the fence structure is flexible and not rigid, the damage to the fence during most rock impacts is only slight. In many cases the decrease in rock velocity after its impact with the fence is sufficient so that the rock will harmlessly come to rest shortly after impacting the fence, and not enter the highway. In extreme cases where very large rocks (over 2000 lbs) moving with high velocity hit the fence, the fence capacity is exceeded. In this situation the hanger connection at the top of the steel rod that passes through the center of attenuator is designed to break. This failure results in the loss of an attenuator column but not the

complete breakdown of the fence structure. This design feature allows the fence to be repaired easily, with the simple reattachment of a new attenuator column [2].

The numerical model reported herein, provides a technique that can be used in conjunction with experimental methods to estimate the fence capacity. The present study determines the effects of varying fence design and rock impact parameters on the magnitudes of the relevant dynamics response parameters. For example, the dynamic impact calculations study the effects of different rock sizes and rock velocities on particular fence configurations. Fence response parameters of particular importance include; (i) the forces in the hanger connection and the overhead and bottom cables, and (ii) the decrease in rock velocity due to impact.

The numerical procedure developed to perform this dynamic impact simulation is based upon the DEM. This procedure solves the nonlinear coupled dynamic equations of motion for the idealized fence structure and the impacting rock. The DEM model assumes that the fence structure can be idealized as a system of connected rigid bodies, and the rock as an impacting rigid body. The dynamic fence-rock impact conditions are modeled with a penalty formulation and an automatic contact detection algorithm. This numerical procedure utilizes an explicit time stepping scheme to solve the discretized equations of motion.

1.1 The Prototype Fence Structure and Impacting Rocks

A typical fence structure, similar to those presently being investigated, is shown in Fig. 2. Cylindrical column attenuator masses are connected to a steel wire overhead cable through hanger attachment cables. These column masses consist of layers of used truck tires on their rims that are threaded onto a vertical steel rod. The introduction of the bottom cable connection ensures that the combined mass of all attenuators is active during an impact. It should be noted that any slack in the bottom cable results in a delayed displacement action between attenuators. The area of the bottom cable is approximately one quarter of the area of the main overhead cable with the same modulus of elasticity as the overhead cable. The bases of the attenuator columns are close to the ground to capture low falling rocks. In some cases the attenuator columns are of different lengths to adapt to the uneven profile of the terrain.

The sizes of the most likely impacting rocks range between 500 lbs to 1500 lbs. Corresponding impact rock velocities vary between 50 and 70 ft/s. It should be noted that larger impacting rocks that are over 2000 lbs in weight are likely to cause significant fence damage, and exceed the fence capacity.

1.2 The Discrete Element Method

Discrete element methods are a family of related numerical techniques specifically designed to solve problems in applied mechanics, which exhibit gross discontinuous, material and geometrical, behavior. For example, many DEM's are used to analyze systems

of interacting rigid or deformable bodies undergoing large dynamic or pseudo static motion, governed by complex constitutive behavior. It should be noted that the solutions to problems of this type are often intractable by conventional continuum based methods such as finite element, finite difference and boundary element procedures.

A typical discrete element algorithm includes the following features:

(i) an automatic contact detection scheme which can recognize new contacts as the simulation progresses, and update the contact topology appropriately,
(ii) a contact force model to determine the forces acting between interacting bodies, and
(iii) a time integration scheme to solve the governing equations of motion, which allows for finite displacement and rotation of the discrete bodies within the system.

Applications of DEM's include; the mechanical modeling of granular media, failure analysis of brittle materials (ceramics, rocks, ice, etc.), mechanical behavior of fractured and jointed rock masses, and discrete simulation of compaction in material processing of ceramics and powder technologies [3,6]. More recently, discrete elements have also been applied to continuum structural mechanics problems, which include large displacement dynamic analysis of elasto-plastic beams [4], and deep-ocean mining pipes [5].

2.0 THE FENCE MODEL

The modeling aspects and assumptions of the discrete element model, namely the rigid body dynamics of the fence and rock, the cable behavior, the rock/attenuator impact interaction model and the numerical integration of the dynamic equations of motion are discussed below.

2.1 Rigid Body Dynamics of Attenuator Columns and Rock

The attenuators and the impacting rock are both represented by three-dimensional rigid bodies. The local elastic or plastic deformation that occurs in the vicinity of the point of contact during the impact is accounted for within the contact force law. Details of the contact model are given in a subsequent section of this paper. The fence attenuator columns are modeled as circular cylinders, and the impacting rock as a sphere. The kinematics of the fence attenuator columns and the rock is assumed to be planar. The dynamic motion of the fence attenuators and rock are therefore, confined to the x, y plane (see Fig. 2b).

2.2 Rigid Body Boundary Geometry

A superquadric geometrical formulation is used to describe the two- dimensional surface geometry of the outline of attenuators and the rock. This geometrical surface model can be used to describe any shape, from an ellipse to a rectangle. The boundary shape of the

two-dimensional body is defined by a number of boundary nodal points on the super ellipse:

$$(x/a)^n + (y/b)^n = 1 \qquad (1)$$

Notes: (i) x, y are principal local centroidal coordinates for the super ellipse, and (ii) the parameters a, b and n define the bounding dimensions and shape of the super ellipse.

The current positions of these boundary nodes are then utilized to check for geometrical contact or overlap with neighboring bodies. This check is performed with a simple algebraic calculation of an inside-outside function. It should be noted that the superquadric representation provides analytical formulae for the convenient computation of the outward normal and curvature at any point on the boundary of the body. For further details, the reader is referred to [1].

2.3 Impact Geometry Conditions

It is assumed that the rock hits the central portion of the fence (Fig. 1). This assumption allows the use of symmetry. Furthermore, since the average dimension of the rock is approximately equal to the diameter of an attenuator, if the fence contains an odd number of attenuators, the rock impacts the central attenuator only, otherwise, the rock impacts the two central attenuators symmetrically and the impact loads are equally distributed between the two central attenuators. In this situation the two central attenuators are assumed to move together.

2.4Cable Connections

The sections of cable connecting adjacent attenuators are idealized as massless cable elements with linear elastic or perfect elastic-plastic material behavior. The pre-impact position of the overhead cable is defined as the static equilibrium shape due to the self weight of the attenuator columns. This position is simply computed by a direct application of the static equilibrium equations for the fence. These cable elements transmit tension only and may become slack if appropriate kinematic conditions occur. Note, that since the attenuators are constrained to move only in the x, y (Fig. 2b) plane, the z-coordinates of the ends of the cable elements do not change.

2.5 Dynamic Contact Forces

The dynamic contact forces generated during the impact are determined with a penalty formulation. The penalty method employs a contact "element" at the point of impact between the two bodies that is defined by a combined concentrated stiffness and damping element. This contact "element" produces forces that depend upon the current penetration or overlap distance and relative impact velocity between the impacting rock and the attenuator at the point of impact. These forces are applied in an equal and opposite

manner to the rock and the attenuator. Further details of the penalty approach are given in a subsequent section of this report.

Note, that only the central attenuator(s) is impacted. The other attenuators act as slaves that move only because of forces transmitted through cables connecting adjacent attenuators. Furthermore, note that contact forces between adjacent attenuator columns are neglected, since they are small compared with the impact force between the central attenuator and the impacting rock.

3.0 COMPUTATIONAL DETAILS OF FENCE MODEL

3.1 Attenuator Equations of Motion

The equations of motion for the i^{th} fence attenuator, assuming that the dynamic motion is planar and confined in the x-y plane are given by:

$$m_i \ddot{x}_i = \Sigma F_{xi} \tag{2}$$

$$m_i \ddot{y}_i = \Sigma F_{yi} \tag{3}$$

$$I_i \ddot{\theta}_i = \Sigma M_i \tag{4}$$

for i = 1,2,...N, where N_a is the total number of fence attenuators, and N is defined as $N = (N_a + 1)/2$. See Fig. 3 for details of the attenuator identification numbering scheme. The corresponding resultant loading terms in equations (2),(3) and (4), are:

$$\Sigma F_{xi} = \overline{T}_{xi} + \overline{B}_{xi} + P_{xi} \tag{5}$$

$$\Sigma F_{yi} = \overline{T}_{yi} + \overline{B}_{yi} + P_{yi} - m_i g \tag{6}$$

$$\Sigma M_i = \overline{B}_{xi}\, b\cos\theta_i + \overline{B}_{yi}\, b\sin\theta_i + \overline{T}_{xi}\, a\cos\theta_i + \overline{T}_{yi}\, a\sin\theta_i + P_{xi}\, \Delta y_i + P_{yi}\, \Delta x_i \tag{7}$$

where $\overline{T}_{xi}$ and $\overline{T}_{yi}$ are the global x- and y- components of tension forces induced at the top overhead cable connection, $\overline{B}_{xi}$ and $\overline{B}_{yi}$ are the global x- and y- components of tension forces induced at the bottom cable connection, P_{xi} and P_{yi} are the global x- and y-components of the contact forces generated by the rock attenuator impact, and g is the

gravitational constant. For the i^{th} attenuator the following parameters are defined: m_i is the mass, I_i is the mass polar moment of inertia with respect to the centroid, g is the gravitational constant, x_i and y_i are the global centroidal coordinates, and θ_i is an angular coordinate defining the axial direction of the attenuator (see Fig. 4). The distances of the top and bottom cable connections with respect to the attenuator centroid are defined by a and b, respectively. The global x- and y- coordinates of the point of contact of the rock with the attenuator measured with respect to the attenuator centroid are defined by Δx_i and Δy_i. Note, that if N is even, the mass and moment of inertia terms in equations (2) through (4), for i=1, are doubled. This modification is required because of the assumed symmetrical impact geometry.

3.2 Rock Equations of Motion

The corresponding equations of motion for the rock are:

$$m_r \ddot{x}_r = P_{xi} \tag{8}$$

$$m_r \ddot{y}_r = P_{yi} - m_r g \tag{9}$$

$$I_r \ddot{\theta}_r = P_{yi} \Delta x_r - P_{xi} \Delta y_r \tag{10}$$

where m_r is the mass of the rock, I_r is the rock mass moment of inertia with respect to its centroid, and Δx_r ,Δy_r are the global x- and y- coordinates of the point of contact of the rock with the attenuator, with respect to the centroid of the rock.

3.3 Top Cable Attachment Forces

In Fig. 5, the top overhead cable segment with end points T_i and T_{i+1} between attenuators i and i+1 is shown. In a coordinate system with the origin at point T_i, the coordinates of point T_{i+1} are denoted by (x_{i+1}, y_{i+1}, d_i), where d_i is the horizontal distance between attenuators i and i+1, which is constant because of the assumption of planar kinematics. At time t = 0, the initial position of the point T_{i+1} with respect to point T_i is given by:

$$(0, y_{i+1}, -d_{i+1}) = (0, y_i, 0) + (0, H, -d_{i+1}) \tag{11}$$

where $H = h_{i+1} - h_i$. Note that the initial vertical positions, h_i, which define the pre-impact configuration are calculated from static equilibrium as discussed previously. The initial unstretched length of the cable segment at time t = 0 is computed from:

$$\ell_{oi} = (d_i^2 + H^2)^{1/2} - T_{oi} / k_i \tag{12}$$

where k_i is the axial stiffness of the cable segment, and T_{oi} is the initial tension of the cable segment in the initial equilibrium condition. The current length of the cable segment at time t is given by:

$$\ell_i = (x_i^2 + y_i^2 + d_i^2)^{1/2} \tag{13}$$

The tension in the cable segment at time t is computed from:

$$T_i = \begin{cases} k_{oi}(\ell_i - \ell_{oi}) & \text{for } \ell_i \geq \ell_{oi} \\ 0 & \text{for } \ell_i < \ell_{oi} \end{cases} \tag{14}$$

Note, that the above equation models cable slack correctly and non-physical compressive forces cannot be transmitted. The corresponding global x- any y- components of the cable tension are given respectively by:

$$T_{xi} = T_i x_i / \ell_i \quad \text{and} \quad T_{yi} = T_i y_i / \ell_i \tag{15}$$

The resultants global x- and y- components of forces acting on the i^{th} attenuator due to the tension at the top cable connection induced in the cable segments between the $(i-1)^{th}$, i^{th} and $(i + 1)^{th}$ attenuators is determined from:

$$\overline{T}_{xi} = T_{xi} - T_{xi-1} \quad \text{and} \quad \overline{T}_{yi} = T_{yi} - T_{yi-1} \tag{16}$$

It should be noted that for the first attenuator (i=1), $T_{xo} = T_{yo} = 0$, and because of symmetry the resultant forces T_{xi} and T_{yi} are doubled.

3.4 Bottom Cable Attachment Forces

The previous analysis for the computation of the top overhead cable forces is applicable to the bottom cable forces with the following minor modifications:

(i) the axial cable stiffness for the bottom cables should be changed accordingly, and

(ii) the initial tension in the bottom cables is zero, and there is a significant amount of slack cable length which must be taken up before any tensile forces are transmitted to the attenuators.

Condition (i) requires that the axial stiffness of the bottom cable is doubled because of the double cable wrapping in the fence design (see Fig. 2a).

Condition (ii) is accounted for by modifying the corresponding form of the equation (12) for the unstretched cable length by setting $T_{oi} = 0$ and by increasing the unstretched length by a user-defined slack cable length.

3.5 Contact Forces

An accurate representation of the dynamic impact forces, stresses and strains generated during the fence-rock impact event would require a detailed non-linear dynamic impact analysis. This could be performed with a finite element calculation in which the rock and the attenuators would be idealized as deformable bodies. However, since only the energy transfer mechanism between the rock and the fence is of primary interest, a simple dynamic contact model can be used. The normal contact element model is comprised of a linear spring stiffness and viscous damper, connected in parallel, that acts in the contact normal direction at the instantaneous point of contact, as shown in Fig. 6a. Behavior in the contact shear direction is defined by a shear contact element model consisting of a linear spring stiffness and a slider that simulates a simple Coulomb dynamic friction model (see Fig. 6b). Note, that the contact normal and shear directions are defined by the boundary geometry of the body with the smoothest tangent plane at the point of contact. The normal and shear contact element model are active only when the discretized boundaries of the rock and the attenuator penetrate each other.

The normal instantaneous contact force, F_n, is defined by:

$$F_n = \begin{cases} k_n \delta_n + c \dot{\delta}_n & \text{for } \delta_n \geq 0 \\ 0 & \text{for } \delta_n < 0 \end{cases} \tag{17}$$

where, k_n is the normal contact stiffness, c is the normal contact viscous damping coefficient, and δ_n is the normal penetration distance at the point of contact.

The shear instantaneous contact force, F_s, is given by:

$$F_s = \begin{cases} k_s \delta_s & \text{for } k_s|\delta_s| < \mu |F_n| \text{ and } \delta_n > 0 \\ \mu F_n & \text{for } k_s|\delta_s| \geq \mu |F_n| \text{ and } \delta_n > 0 \\ 0 & \text{for } \delta_n < 0 \end{cases} \tag{18}$$

where, k_s is the shear contact stiffness, δ_s is the shear slip distance at the point of contact and μ is the dynamic coefficient of friction between the rock and the attenuator.

Note: A suitable value of the normal contact stiffness k_n is specified by the user by limiting the maximum penetration, or overlap, between the surfaces of the impacting two bodies to a predefined value. Typically, this maximum penetration is defined as a small fraction of the average body dimension of the contacting bodies. For example, this fraction is usually between 0.01 and 0.05. An estimate of k_n can simply be determined with an approximate energy calculation for the impacting bodies.

For fence-rock impact studies the normal contact stiffness k_n should be determined by prescribing an approximate maximum overlap between the rock and attenuator elements. A facility for this has been included in the DEM computer model and is mentioned in Appendix II of this report. In the analyses performed in Appendix I for double layer fences an overlap of six inches was prescribed.

3.6 Restitution Model

In the discrete element numerical model, the energy loss due to impact is simulated with a viscous damper which acts at the point of impact, P, in the contact normal direction. The normal viscous force, F_n, in this damper, which is the second term in the normal contact force equation (17), is given by:

$$F_c = c\,\dot{\delta}_n \tag{19}$$

where $\dot{\delta}_n$ is the normal component of the relative velocity of the fence with respect to the rock at the point of contact, and is defined by:

$$\dot{\delta}_n = (\vec{v}_{Pf} + \vec{v}_{Pr}) \cdot \hat{n} \tag{20}$$

Note, that $\hat{n}$ is the unit outward contact normal direction at the point of impact, P, and $\vec{v}_{Pf}$ and $\vec{v}_{Pf}$ are the velocities of the fence and the rock during the impact, respectively, and c is the normal contact viscous damping coefficient as defined in equation (17).

In a dynamic impact between two bodies, the energy loss can be approximately modeled with a simple restitution model which requires e, the coefficient of restitution, to be known a priori via experimental data. Due to lack of available quantitative data concerning the impact energy losses during a fence-rock impact situation this simple model is appropriate. However, in order to apply the normal contact force law, equation (17), a relationship

between the viscous damping coefficient c, and the coefficient of restitution e, is required. For this purpose, a simple approximate relationship between the viscous damping coefficient, c, and the coefficient of restitution, e, can be derived by assuming that the rock and the attenuator are approximated as two particles of mass m_r and m_f, respectively. This results in the relationship:

$$c = 2\ln(1/e)\left[k_n m_r m_f/(m_r+m_f)\right]^{1/2}\Big/\left[\pi^2+\left(\ln(1/e)\right)^2\right]^{1/2} \qquad (21)$$

where k_n is the normal contact stiffness at P, the point of impact.

It should be noted that the use of equation (21) is only approximate when applied to a non-central impact between a spherical rock and a cylindrical attenuator. Some numerical experimentation, therefore, is usually required to obtain the precise value of the viscous damping coefficient which corresponds to a specified value of the coefficient of restitution.

3.7 Time Stepping Algorithm

The above equations of motion, (2), (3) and (4), which describe; (i) the translational rigid body motion of the center of mass for each attenuator element, and, (ii) the rotational motion of each element, can be written in the generalized form:

$$M_i^k \ddot{q}_i^k = F_i^k, \quad k = 1, 2, 3 \qquad (22)$$

where q_i^k is a generalized coordinate, M_i^k is a generalized mass, and F_i^k is a generalized loading vector.

For a planar rigid body element, the generalized variables are identified as follows:

(i) the generalized coordinates, q_i^1, q_i^2, are the element centroid Cartesian coordinates x_i, y_i, and q_i^3 is the angular coordinate θ_i, of the elements longitudinal or local x-axis,

(ii) the generalized masses, M_i^1, M_i^2 are the element mass m_i,

and M_i^3 is the elements polar mass moment of inertia I_i, and

(iii) the generalized loading vector, F_i^1, F_i^2, are the x,y- components of applied forces acting at the element centroid and

F_i^3 is the applied moment acting at the element centroid.

The solution of the above decoupled dynamic element equations for large rigid body motions is obtained with an updated Lagrangian algorithm. This procedure employs incremental updating of the element centroid kinematic variables. Time integration of the

dynamic element equations is then performed with an explicit central difference time stepping scheme.

The central difference time step update scheme for the generic dynamic equilibrium equation (22), from time t^n to $t^n + \Delta t$, is performed in two parts:

(i) a generalized velocity update for the linear and angular velocity of the center of mass of all the elements, where the generalized velocities, $\dot{q}_i^k$, for a typical element are updated by:

$$^{n+1/2}\dot{q}_i^k = {}^{n-1/2}\dot{q}_i^k + \Delta t^n F_i^k / M_i^k \qquad (23)$$

where the pre-superscripts n-1/2, n, and n+1/2 indicate quantities defined at times $t^n - \Delta t/2$, t^n, and $t^n + \Delta t/2$, respectively, and

(ii) a generalized position update for the coordinates of the center of mass and the local longitudinal axis of all the elements, where the generalized coordinate for a typical element, q_i^k, is updated by:

$$^{n+1}q_i^k = {}^{n}q_i^k + {}^{n+1/2}\dot{q}_i^k \Delta t \qquad (24)$$

The pre-superscripts n and n+1 indicate quantities defined at times t^n and $t^n + \Delta t$.

The numerical stability criteria of this time stepping scheme depends on the maximum frequency of the combined discrete element system, ω_{max}. This gives a time step limitation constraint of the form:

$$\Delta t_{max} < 2 / \omega_{max} \qquad (25)$$

where Δt_{max} is the maximum allowable time step. This criteria can be applied simply with the largest natural frequency of any rigid attenuator element within the fence structure which is an approximate upper bound of ω_{max}. This approximate procedure avoids a costly eigenvalue analysis of the whole discrete element fence idealization.

4.0 DESCRIPTION OF THE DEM SOFTWARE MODULES

The DEM dynamic fence-rock analysis software consists of three major modules:
(i) the computational DEM module (FENCE),
(ii)the geometrical graphics snapshot and animation module (GPLOT), and
(iii)the time history graphics module (HPLOT).

In the DEM computational module, FENCE, the input data contains the following parameters:

(i) fence and rock geometry and mass properties,
(ii) material model and properties for the fence cables,
(iii) impact and restitution parameters between the fence and the rock,
(iv) the initial rock velocity prior to impact, and
(v) control parameters which describe the type and time intervals of the computed results.

This input data is contained in a data file with a user-specified name appended with the extension .DAT.

The computed results are written to three different output data files with a user-specified name appended with the extensions .OUT, .HST, and .GEO, respectively. These output data files are called the printout file, the time history file, and the geometry file, respectively.

The printout file is used directly to verify the input data and for checking purposes by the user. The time history and the geometry results data files are input data for the graphical post-processing modules HPLOT and GPLOT, respectively.

The HPLOT graphics module interactively displays time history plots and produces postscript graphics output. Typical time history data plots include; (i) centroidal kinematics quantities such as position and velocity components for the rock and the attenuator columns, and (ii) forces in the overhead and bottom cable segments, and the attenuator hanger connections.

The GPLOT graphics module is used to display the following geometrical data for the fence-rock system; (i) single snapshots of the fence-rock geometry at prescribed times during the impact, or (ii) animation of the fence-rock motion throughout the impact. Postscript graphics output of the single geometry snapshots can also be produced by GPLOT.

The hard copy graphics output from HPLOT and GPLOT have been used to illustrate the computational results obtained from the numerical analyses presented in the subsequent sections in this paper. It is the opinion of the authors that without graphical output these analyses would be very difficult to perform and interpret effectively.

5.0 VALIDATION PROBLEMS

The following example problems are presented to validate the above described discrete element computational procedure. These calculations illustrate that this numerical approach accurately models; (i) dynamic impact phenomena between rigid bodies, (ii)

large dynamic rigid body motion and translation, and (iii) large elastic deformations of the flexible cables attached to the bodies.

The first example problem consists of a particle of mass m, initially at rest, attached to two unstretched elastic cables of stiffness, k, and length, ℓ, in a horizontal plane (note that the gravitational effects are ignored), being impacted by a particle of mass M with an initial velocity v_o (see Fig. 7). The coefficient of restitution for this impact is defined by e.

The data used for this analysis are as follows:

k = 4 N/m, ℓ = 10 m, m = 1 kg, M = 2 kg, e = 0.5, and v_o = 2 m/s.

The analytical solution for this problem is described by:

$$v_1 = M(1+e)v_o/(M+m) \tag{26}$$

Where v_1 is the velocity of the particle of mass m, immediately after the impact, and

$$v^2(\theta) = v_1^2 - 2k\ell^2(1-\cos\theta)^2/(m\cos^2\theta) \tag{27}$$

where $v(\theta)$ is the velocity of the particle of mass m after the impact at the instant when the cables subtend an angle θ with respect to their initial directions.

The time histories of the x-component of velocity for the particles of masses m and M are shown in Fig. 8. The distance moved by the particle of mass m, after its velocity decreases to zero is computed as 3.826 m and corresponds to an angle θ = 0.365 radians. This is in good agreement with the exact result which can be obtained from equation (27). It should also be noted that the velocity immediately after impact is 1.997 m/s, which compares closely with the analytical value of 2.0 m/s, predicted by equation (26). This result validates the viscous damper - restitution coefficient equation stated in equation (21), previously.

The second validation problem consists of a single cylindrical attenuator being impacted by a spherical rock moving with an initial horizontal velocity v_o. The cylindrical attenuator is pin-jointed at its top, and the line of impact is through the center of mass of the attenuator, (see Fig. 9). The superquadric geometrical representation of two-dimensional outline shapes of the spherical rock and the cylindrical attenuators in the subsequent analyses are defined as follows:
(i) the rock geometry is defined by a circular boundary shape with twelve equally spaced nodes, and
(ii) the fence attenuator geometry is defined by a boundary shape with four nodes at the corners of the rectangular boundary.

The attenuators mass, moment of inertia with respect to the center of mass, vertical height and radius are defined by m, I_G, ℓ and r, respectively. The mass of the rock is M, and the coefficient of restitution is e. The data for this analysis are given as:

m = 14.92 slugs, ℓ = 8 ft, I_G = 85.42 slug-ft^2, r = 1.2 ft,
M = 37.23 slugs, v_o = 5 ft/s and e = 0.5.

The analytical solution for this problem is given by:

$$v_1 = M(1+e)(\ell^2/4)/\left[I_G + (M+m)\ell^2/4\right] \tag{28}$$

where v_1 is the speed of the center of mass of the attenuator immediately after the impact. Note: the corresponding angular velocity is determined by:

$$\omega_1 = 2v_1/\ell \tag{29}$$

The subsequent angular velocity of the center of mass of the attenuator, $\omega(\theta)$, when the angle of the longitudinal axis of the attenuator with respect to the vertical direction is θ, is defined by:

$$\omega^2(\theta) = \omega_1^2 + 2mg\ell(\cos\theta - 1)/\left(I_G + m\ell^2/4\right) \tag{30}$$

The numerical results of the dynamic impact simulation are given in Figs. 10 and 11. Fig. 10 shows snapshots of the geometry of the rock and the attenuator during the dynamic impact simulation. A time history of the horizontal component of velocity of the rock and the attenuator during and after the impact is shown in Fig. 11. The computed horizontal components of the rock and the attenuator immediately after the impact are 2.36 ft/s and 4.85 ft/s respectively, which are in close agreement with the exact solution. The maximum angle of rotation of the attenuator after the impact was computed to be 0.503 radians which agrees with the analytical value to three significant figures. This analytical result can be computed from equation (30).

6.0 ROCK IMPACT STUDIES

6.1 Model Dimensions and Properties

A full size fence model is used to study the dynamic response of the fence due to impacting rocks. A similar full size prototype fence has been built by the Colorado Department of Highways (CDOH). Limited experimental data, which is mainly qualitative, has been obtained from this fence structure by the CDOH. Dimensions and material properties for this numerical idealization are described in Fig. 2 and Table 1. In the present computer model two idealized material models for the cable behavior have been

implemented. The first is a simple linear elastic model, and the second is a perfect elastic-plastic model. These models were selected, since more precise cable data for the prototype fence was not available. It should be noted that more realistic material models for the cable can be readily inserted into the present algorithm. For example, a constititutive model with time dependent stiffness properties which accounts for cable life [7], could be implemented.

6.2 Simulation Results

A series of analyses were performed which included the following possible combinations: (i) two rock sizes, (ii) the two material models, (iii) different rock impact heights, (iv) different bottom cable slack conditions, and (v) no bottom cable. Each computer run required approximately 100,000 time steps with $\Delta t = 2 \times 10^{-6}$ seconds. Each analysis required about 15 minutes, using an Intel CPU based 80486, 33 MHz microcomputer.

Tables 2 and 3 summarize the computed results for the 600 lb. rock, and the 1200 lb. rock, respectively. The calculations include the maximum forces in the fence cable segments and the attenuator hanger connections, and the final rock velocities after the impact. The results quoted are for analyses performed with; (i) the linear elastic cable model, and (ii) the perfect elastic-plastic cable model. Note, that the results for the perfect elastic-plastic model are quoted in parenthesis in Tables 2 and 3. A bottom cable slack of 0.5 ft. is assumed. The first column in Table 2 indicates the vertical variation of the rock impact position with respect to the attenuator centroid.

Figures 12 through 15 show detailed geometry snapshots and time history plots for an impact situation, when the rock impact location coincides with the centroid of the attenuator. Figs. 12 and 13 show snapshots of the fence-rock geometry during the impact for the 600 lb rock, with a bottom cable (0.5 ft slack), and without bottom cable, respectively. Figures 14 and 15 illustrate time histories for the primary design parameters, namely, attachment force, forces in top and bottom cable, and the rock horizontal velocity. These results were computed for both rock sizes and cable material models. The computed results presented in Tables 2 and 3, and the time history data in Figs. 14 and 15 are discussed below.

A series of further analyses were performed for 600 lb and 1200 lb rock impacts against a single layer fence structure. In these simulations the bottom fence cable was analyzed under the two following conditions: (i) 0.0 ft. slack, and (ii) 0.25 ft. slack The maximum forces in the top overhead cable and top joint at the central attenuator are quoted in Tables 4 and 5. From the results of the analyses it was concluded that different slack bottom cable lengths cause only minor differences in the overall impact behavior and mechanical response of the fence. For example in the simulations with slack cables short duration force spikes in the fence impact force time histories were noted.

6.3 Observations

From the computational results of the analyses which are summarized in Table 2 and 3, the following general observations can be made: (i) for a fence with a bottom cable: elastic cable forces tend to reach a maximum when the impact takes place near, and above, the attenuator centroid, and (ii) for a fence without a bottom cable the elastic cable forces tend to increase with impact height. In both fences, with or without bottom cables it is observed that the rock post-impact velocity decreases with increasing impact height.

The time histories presented in Figs. 14 and 15 give more detailed insight to cable behavior and rock velocity characteristics for a particular impact. Relevant observations are summarized as follows:

(i) There exists a significant difference in the fence cable forces computed, assuming elastic and perfect elastic-plastic cable behavior, respectively. It is noted that the elastic-plastic material model predicts minor yielding which "cushions the impact", and reduces the unrealistically high impact peak forces in the cables obtained by the elastic cable model (see Figs. 14b, and 14f).

(ii) The slack in the bottom cable produces force spikes introducing further impacts to the attenuators. Slack in the bottom cable causes a delayed sequence of impulsive cable forces which act between adjacent attenuators This phenomenon leads to force spikes in the cable forces (see Figs. 14c, and 14g).

(iii) The fence with a bottom cable produces multiple impacts between the attenuator and the rock, thus, reducing the rock velocity gradually in stages.

(iv) Minor plastification takes place in the top overhead cable mostly during the first impact between the rock and the attenuator (see Figs. 14i and 15i).

7.0 CONCLUDING REMARKS

A powerful numerical modeling tool has been developed for the non-linear dynamic impact modeling of a flexible rockfall prevention fence. An approximate three-dimensional impact analysis has been performed in an effective manner with a new two-dimensional DEM model. In this model the fence and rock kinematics are assumed to be planar, whereas the cable stiffness effects are modeled in a three-dimensional manner. Nonlinear cable effects have also been included.

The DEM simulation procedure has been mathematically validated and applied to a series of full scale fence-rock impacts with varying design parameters. The numerical results for this series of impact simulations predict the maximum forces generated within the fence cables during a rock impact event. Corresponding predictions of post impact rock velocities have also been made. These initial calculations presented here illustrate the ease with which a designer can evaluate the effects of varying different fence design parameters on the fence capacity. It is hoped that further use of this numerical model, in conjunction

with additional experimental data, will enable the design engineer to improve upon the current methodology employed in the design of flexible rockfall prevention fences.

8.0 ACKNOWLEDGMENTS

The authors wish to acknowledge the financial support of this research work by the Colorado Department of Highways. The authors would also like to thank Robert Barrett, Richard Griffin and Micheal McMullen at CDOH, for their continued interest and helpful discussions during the course of this work.

9.0 REFERENCES

1. Barr, A.H.,(1981) "Superquadrics and Angle-Preserving Transformations", IEEE, Computer Graphics and Applications, Vol. 1, pp. 1-20.

2. Colorado Department of Highways (CDOH), (1992) "Rockfall Attenuator Fence Testing and Analysis", Internal CDOH Report.

3. Greening, D., Mustoe, G.G.W. and DePorter, G.L., (1989) "Discrete Element Modeling of Ceramics Processing", Proceedings of 1st U.S. Conf. on Discrete Element Methods,(Mustoe, G.G.W., Henriksen, M., and Huttelmaier, H.P., Eds.), Sponsored by National Science Foundation, Golden, CO., October.

4. Mustoe, G.G.W., (1992), "A Simplified Discrete Element Method for Large Displacement Plasticity Beam Analysis", Proceedings of 2nd International Conference on Computational Plasticity, Barcelona, Spain, April.

5. Mustoe, G.G.W., Huttelmaier, H.P. and Chung, J.S. (1992), "Assessment of Dynamic Coupled Bending-Axial Effects for Two-Dimensional Deep-Ocean Pipes by the Discrete Element Method", International Journal of Offshore and Polar Engineering (accepted for publication).

6. Thornton, C.,(1989) "Application of DEM to Process Engineering Problems" , Proceedings of the 1st U.S. Conf. on Discrete Element Methods", (Mustoe, G.G.W., Henriksen, M. and Huttelmaier, H.P., Eds.), Sponsored by National Science Foundation, Golden, CO., October.

7. Wire Rope Technical Board, (1990) "Wire Rope Users Manual", Third Edition, American Iron and Steel Institute.

Top Cable Span:	L = 55 ft
Top Cable Sag:	f = 5.5 ft
Modulus of Elasticity:	E = 20,000 ksi
Top Cable Area:	A_{top} = 1.076 in^2
Bottom Cable Area:	A_{bot} = 0.25 in^2 (doubly wrapped)
Tire Height:	t = 8 in
Attenuator Height:	12t = 8 ft
Attenuator Width:	w = 2.5 ft
Attenuator Unit Weight:	γ_{att} = 12.2 lbs/ft^3
Attachment Length:	d = 2.5 ft
Rock Unit Weight:	γ_{rock} = 165 lbs/ft^3
Rock Weight:	600 lbs (case (i))
	1200 lbs (case (ii))
Rock Impact Velocity:	v_x = 65 ft/s (horizontal)
Coefficient of Restitution:	e = 0.4

Table 1. Model Dimensions and Properties

Yc	FORCE IN TOP JOINT 10^4 [lbs]	FORCE IN TOP CABLE WITH BOTTOM CABLE NO SLACK 10^5 [lbs]	FORCE IN BOTTOM CABLE 10^5 [lbs]	V_x - ROCK AFTER IMPACT [ft/sec]
		WITH BOTTOM CABLE SLACK = 0.50 FT.		
-3.0	3.87 (3.95)	1.62 (1.64)	1.41 (1.00)	-4.6 (-5.7)
-1.5	9.02 (5.59)	2.62 (2.00)	1.55 (1.00)	-5.6 (-2.6)
0.0	8.78 (5.83)	2.79 (2.00)	1.55 (1.00)	-1.6 (-6.9)
1.5	6.99 (5.89)	2.39 (2.00)	1.51 (1.00)	-1.1 (-2.5)
3.0	6.64 (5.78)	2.31 (2.00)	0.89 (0.94)	15.5 (8.2)
		NO BOTTOM CABLE		
-3.0	2.76	1.29		-43.7
-1.5	1.02	0.67		-31.7
0.0	2.16	1.10		-23.7
1.5	7.03 (5.91)	2.40 (2.00)		-20.8 (-21.9)
3.0	6.77 (5.83)	2.34 (2.00)		-1.7 (-7.5)

Table 2. Maximum Forces for a 600 lb Rock Impacting a Fence with: (a) with Bottom Cable 0.5 ft. Slack, and (b) without a Bottom Cable

Yc	FORCE IN TOP JOINT 10^4 [lbs]	FORCE IN TOP CABLE WITH BOTTOM CABLE NO SLACK 10^5 [lbs]	FORCE IN BOTTOM CABLE 10^5 [lbs]	V_x - ROCK AFTER IMPACT [ft/sec]
		WITH BOTTOM CABLE,SLACK = 0.50 FT.		
-3.0	7.46 (5.95)	2.5 (2.00)	1.8 (1,00)	-12.9 (-21.1)
-1.5	10.6 (6.19)	3.16 (2.00)	1.78 (1.00)	-11.2 (-14.2)
0.0	13.4 (6.26)	3.7 (2.00)	1.94 (1.00)	-9.7 (-10.8)
1.5	9.77 (6.92)	2.99 (2.00)	2.18 (1.00)	-0.5 (-7.2)
3.0	8.18 (6.85)	2.68 (2.00)	1.47 (1.00)	4.8 (1.3)
		NO BOTTOM CABLE		
-3.0	3.17	1.42		-51.7
-1.5	1.38	0.82		-47.0
0.0	3.15	1.41		-38.6
1.5	9.21 (6.4)	2.89 (2.00)		-35.1 (-34.1)
3.0	9.18 (6.28)	2.87 (2.00)		-16.1 (-17.8)

Table 3. Maximum Forces for a 1200 lb Rock Impacting a Fence with: (a) with Bottom Cable 0.5 ft. Slack, and (b) without a Bottom Cable

Yc	FORCE IN TOP JOINT 10^4 [lbs]	FORCE IN TOP CABLE WITH BOTTOM CABLE NO SLACK 10^5 [lbs]	FORCE IN BOTTOM CABLE 10^5 [lbs]	V_x - ROCK AFTER IMPACT [ft/sec]
-3.0	4.15 (3.61)	1.69 (1.54)	1.29 (1.00)	-5.1 (-5.0)
-1.5	7.97 (5.08)	2.61 (1.94)	1.77 (1.00)	-3.1 (-1.9)
0.0	3.87 (2.69)	1.62 (1.27)	2.09 (1.00)	0.7 (-2.3)
1.5	7.55 (5.89)	2.52 (2.00)	1.64 (1.00)	2.5 (1.71)
3.0	6.54 (5.75)	2.29 (2.00)	1.09 (1.00)	7.1 (6.4)
		WITH BOTTOM CABLE SLACK = 0.25 FT.		
-3.0	5.75 (4.94)	2.10 (1.90)	1.46 (1.00)	-6.4 (-4.2)
-1.5	7.32 (5.77)	2.47 (2.00)	1.39 (1.00)	-0.6 (-2.3)
0.0	10.1 (5.34)	3.06 (2.00)	1.92 (1.00)	-1.2 (-7.2)
1.5	6.99 (5.89)	2.39 (2.00)	1.2 (1.00)	-1.6 (-3.7)
3.0	6.64 (5.78)	2.31 (2.00)	0.99 (0.89)	14.9 (5.5)

Table 4. Maximum Forces for a 600 lb Rock Impacting a Fence with: (a) with Bottom Cable 0.0 ft. Slack, and (b) (a) with Bottom Cable 0.25 ft. Slack.

Yc	FORCE IN TOP JOINT 10^4 [lbs]	FORCE IN TOP CABLE WITH BOTTOM CABLE NO SLACK 10^5 [lbs]	FORCE IN BOTTOM CABLE 10^5	V_x - ROCK AFTER IMPACT [ft/sec]
-3.0	6.4 (4.84)	2.26 (1.87)	1.8 (1.00)	-6.9 (-8.4)
-1.5	11.5 (5.82)	3.33 (2.00)	2.3 (1.00)	-5.9 (-6.7)
0.0	8.01 (3.87)	2.62 (1.68)	2.65 (1.00)	-2.1 (-4.2)
1.5	11.1 (6.68)	3.26 (2.00)	2.03 (1.00)	-0.9 (1.6)
3.0	8.02 (6.33)	2.62 (2.00)	1.55 (1.00)	10.0 (6.4)
		WITH BOTTOM CABLE SLACK = 0.25 FT.		
-3.0	10.4 (6.25)	3.13 (2.00)	1.93 (1.00)	-14.1 (-17.9)
-1.5	9.46 (6.24)	2.93 (2.00)	1.71 (1.00)	-6.6 (-10.6)
0.0	13.0 (5.69)	3.61 (2.00)	2.51 (1.00)	-12.1 (-7.7)
1.5	10.2 (6.68)	3.08 (2.00)	1.87 (2.00)	-1.1 (-5.4)
3.0	8.18 (6.52)	2.66 (2.00)	1.76 (2.00)	9.2 (4.7)

Table 5. Maximum Forces for a 1200 lb Rock Impacting a Fence with: (a) with Bottom Cable 0.0 ft. Slack, and (b) (a) with Bottom Cable 0.25 ft. Slack.

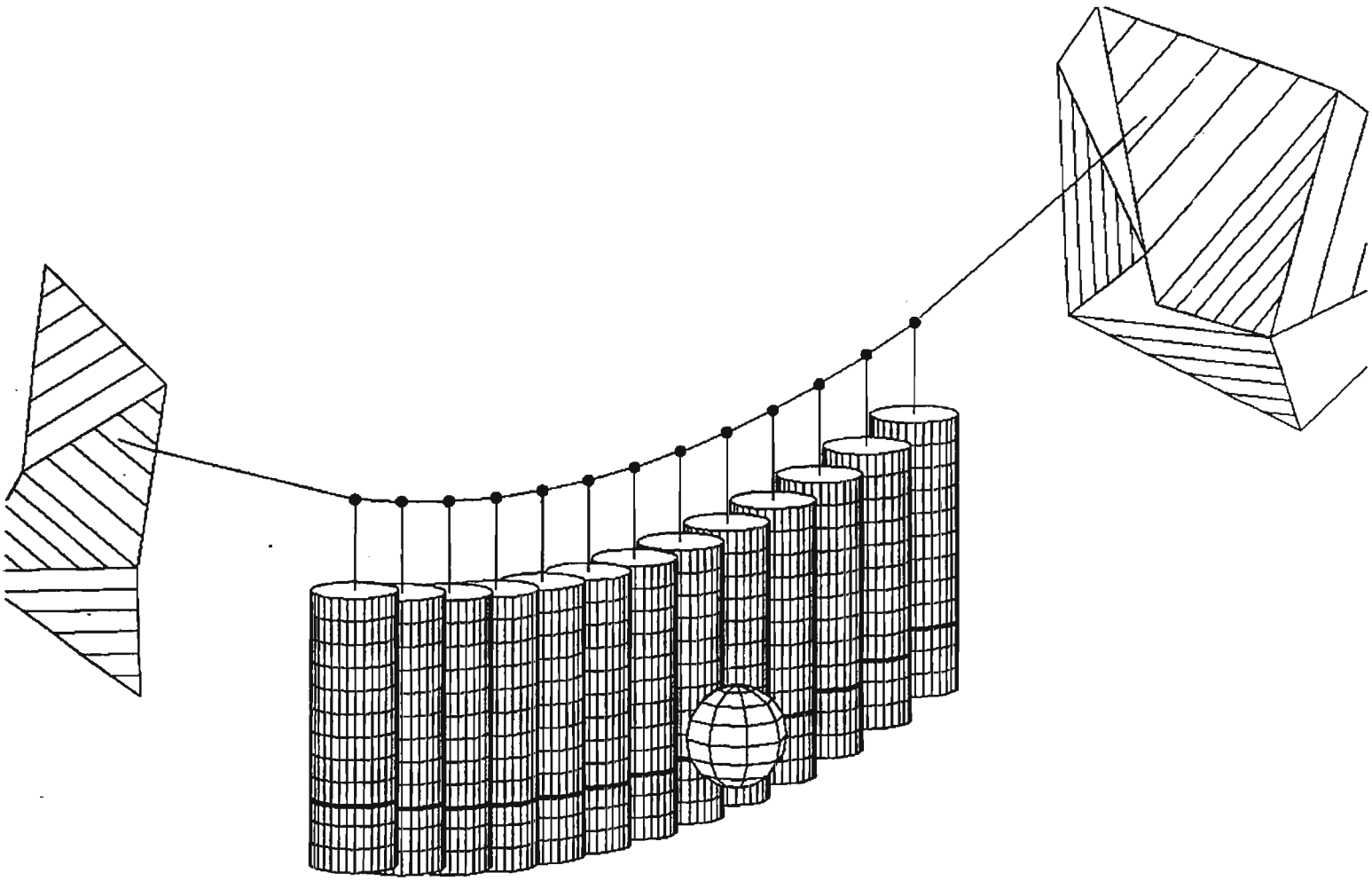

Fig. 1 Fence Structure - Three-Dimensional View

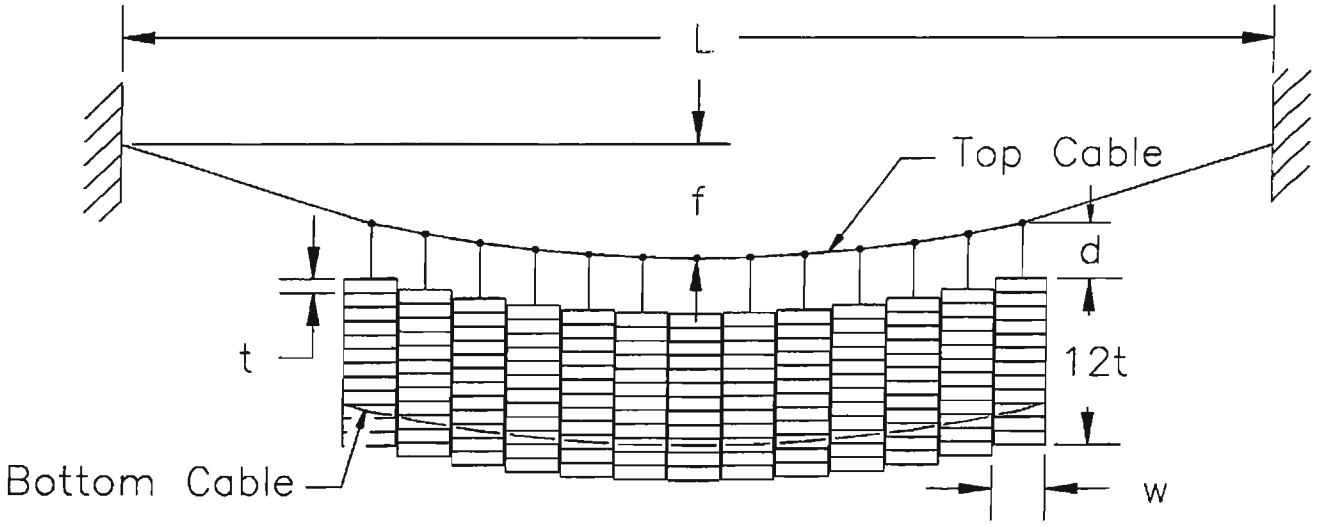

(a)

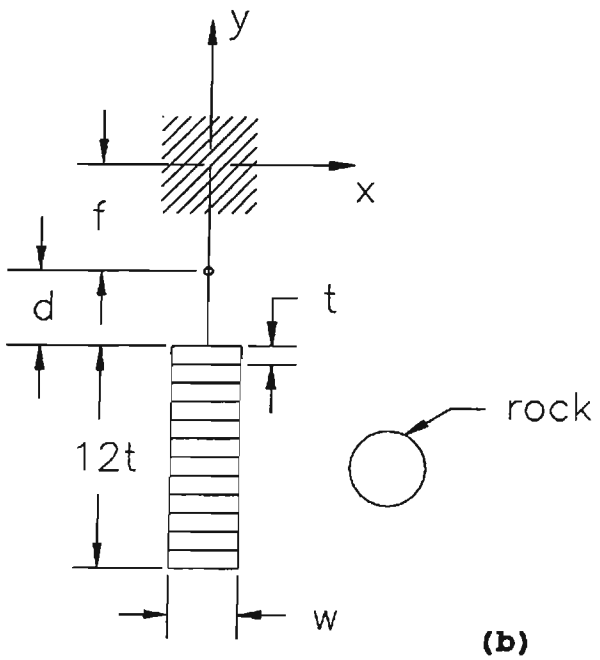

(b)

Fig. 2 Fence Structure: (a) Front View, (b) Side View of a Single Attenuator and Rock

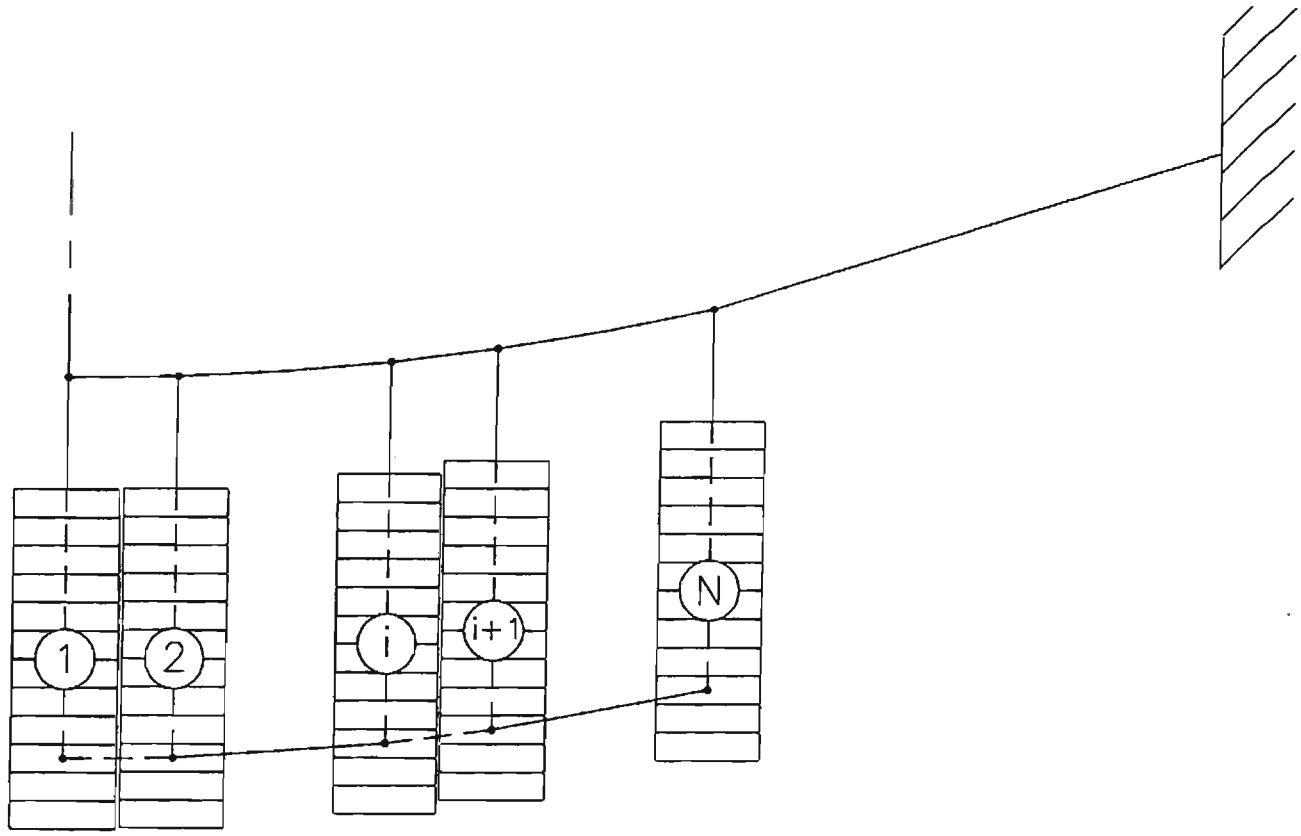

Fig. 3 Attenuator Numbering System

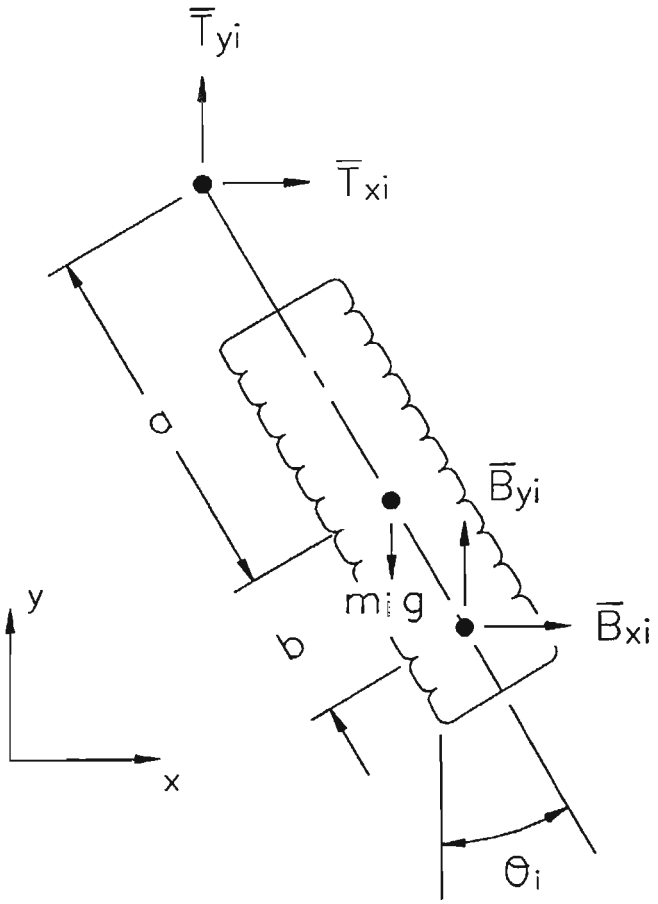

Fig. 4 Attenuator Geometry

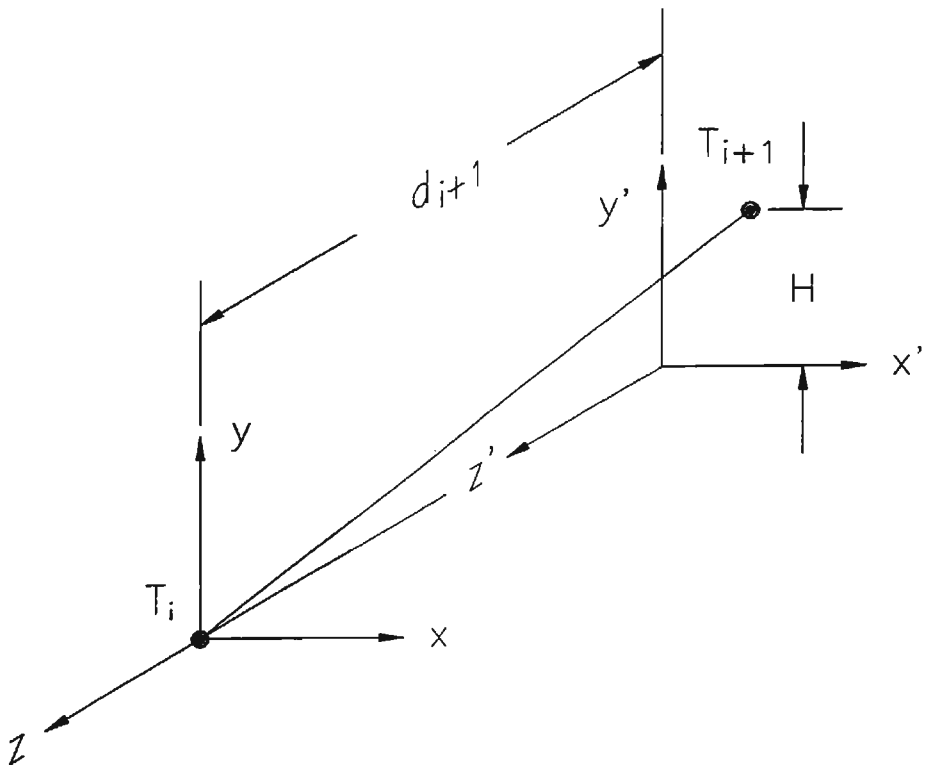

Fig. 5 Cable Geometry - ith Cable Segment

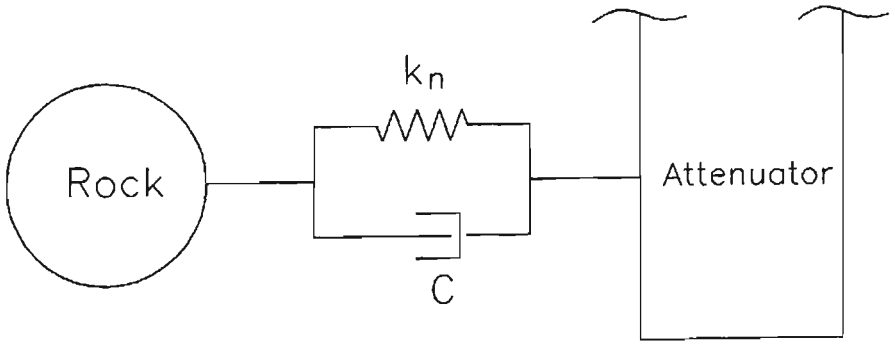

(a)

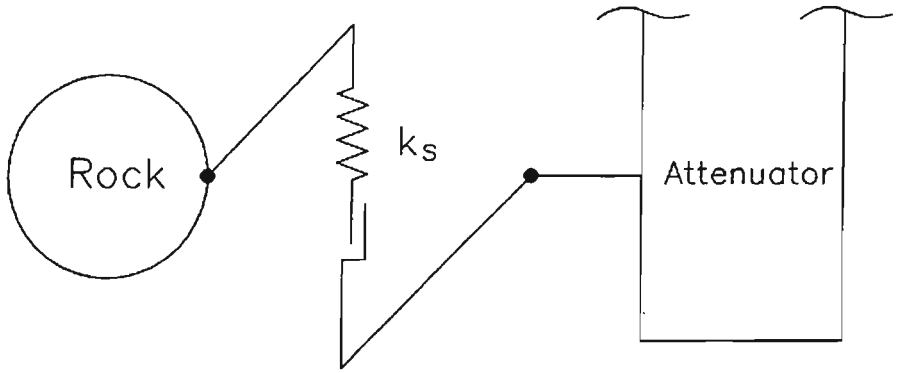

(b)

Fig. 6 Contact Model: (a) "Normal" Contact Element, (b) "Shear" Contact Element

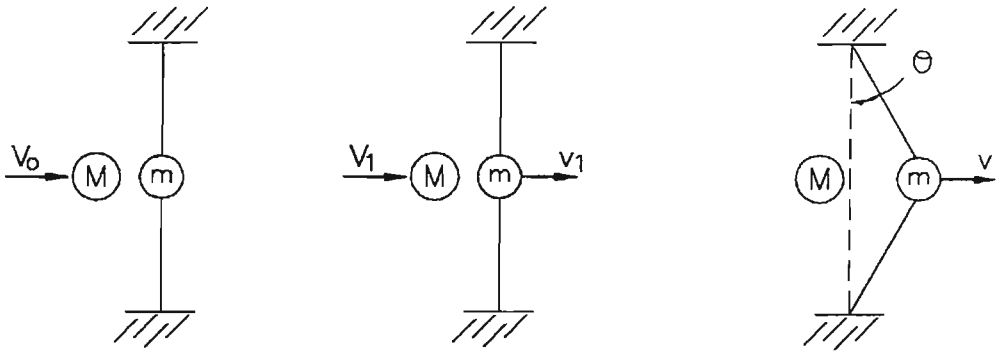

Fig. 7 Particle Impact with Elastic Cables:
(a) Velocities before Impact,
(b) Velocities Immediately after Impact,
(c) Post-Impact Velocities

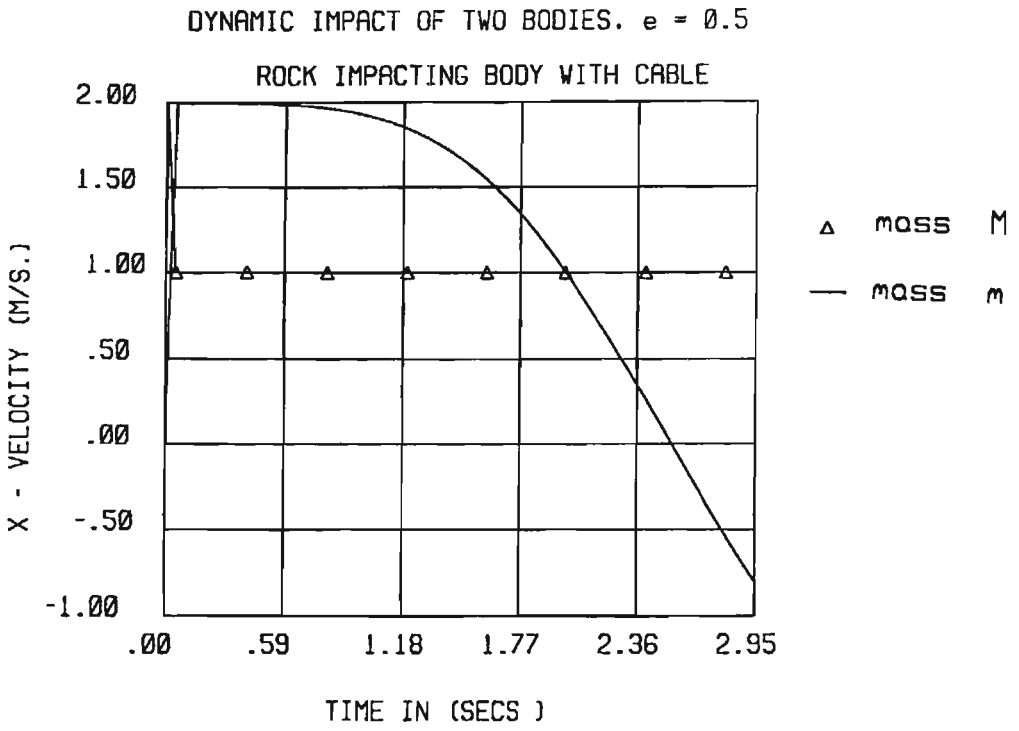

Fig. 8 Particle Impact with Elastic Cables: Velocity Time History

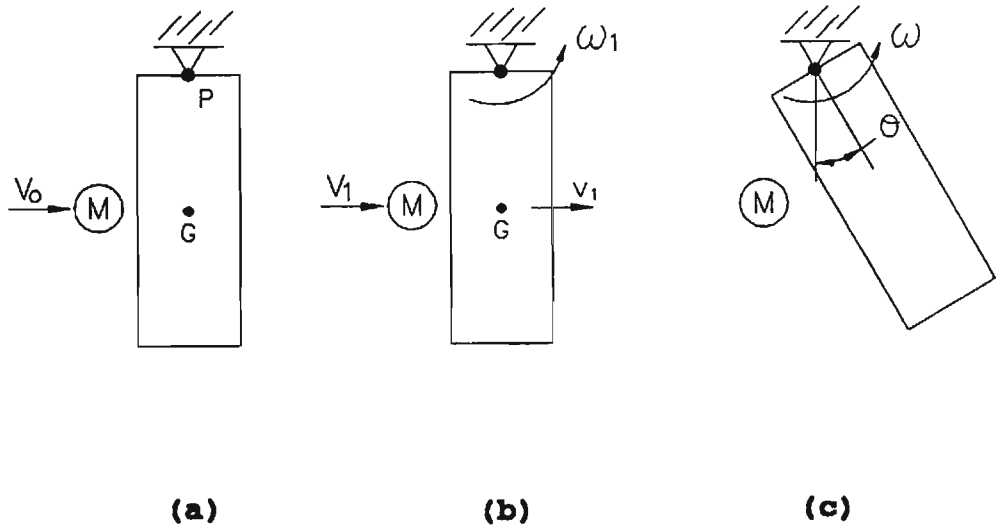

Fig. 9 Pivoted Cylinder Impact Problem:
(a) Velocities before Impact,
(b) Velocities Immediately after Impact,
(c) Post-Impact Velocities

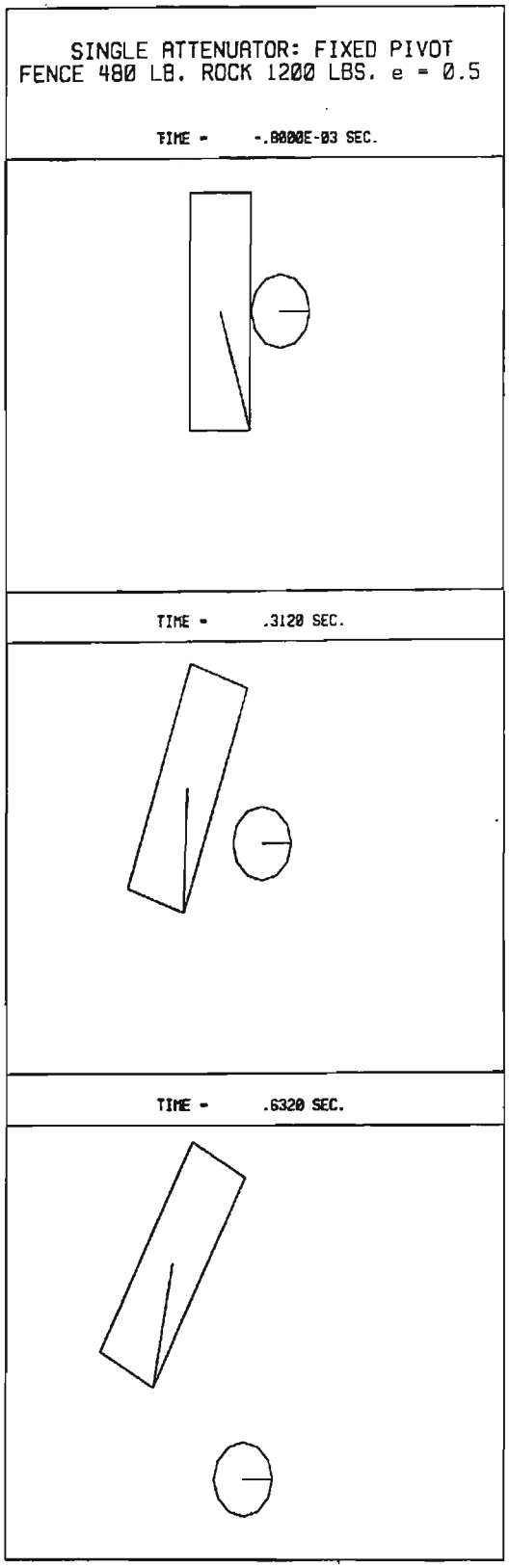

Fig. 10 Pivoted Cylinder Impact Problem: Geometry Plot

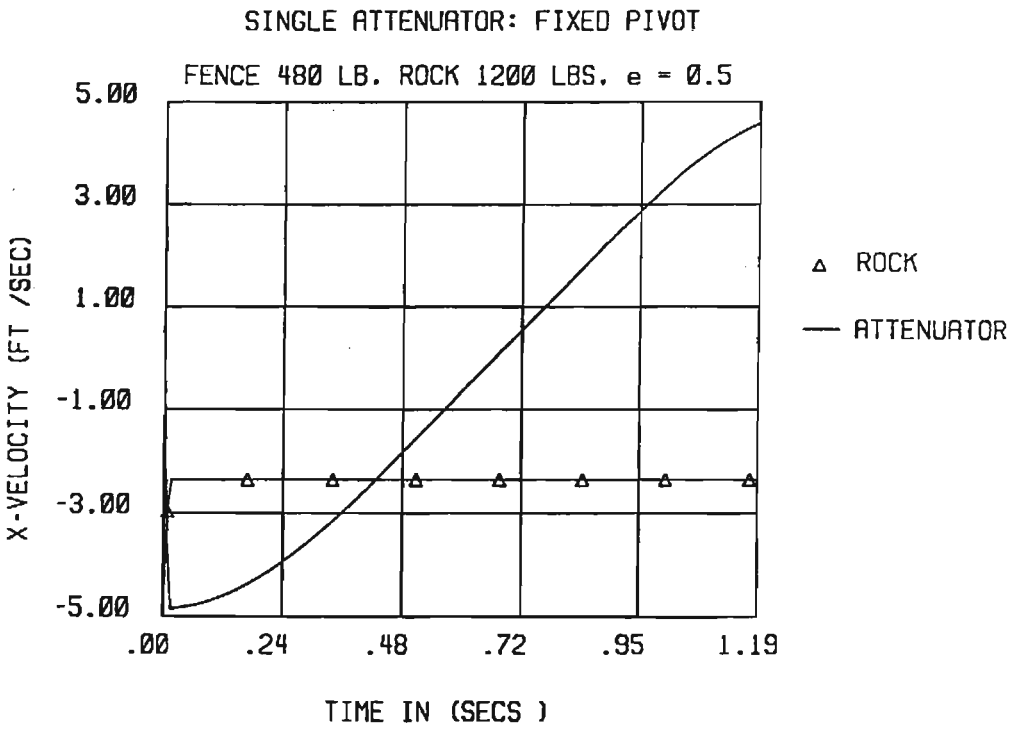

Fig. 11 Pivoted Cylinder Impact Problem: Velocity Time History Plot

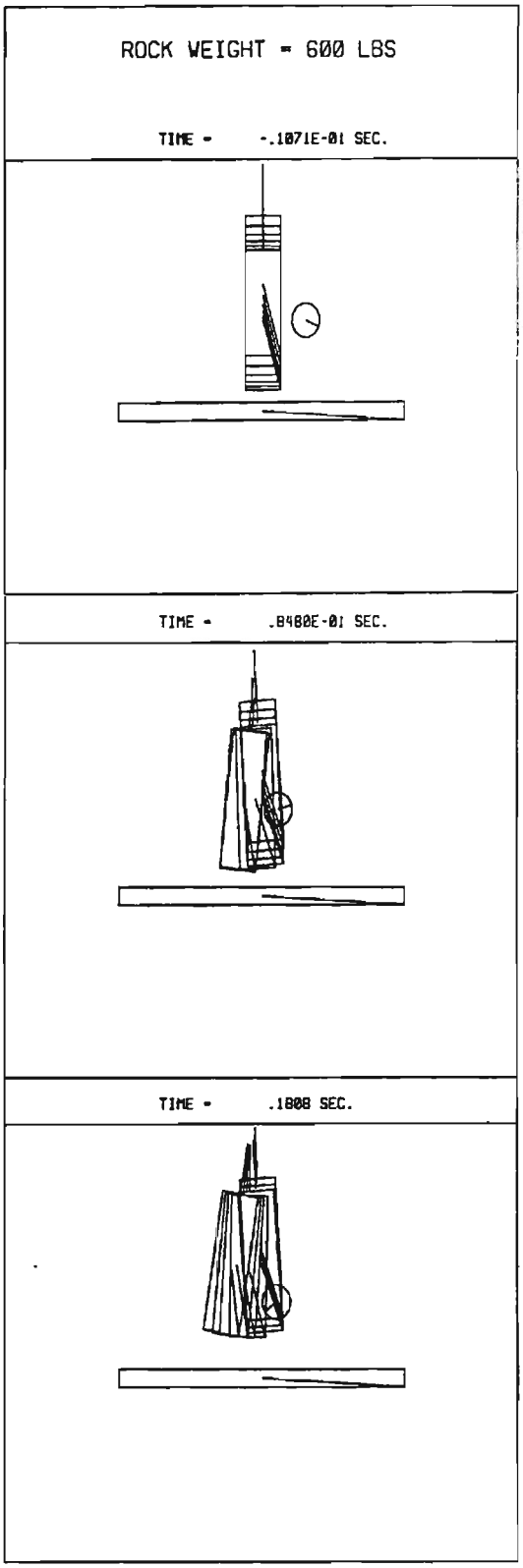

Fig. 12 Impact of 600 LB Rock, with Bottom Cable (Slack = 0.5 FT): Geometry Plot

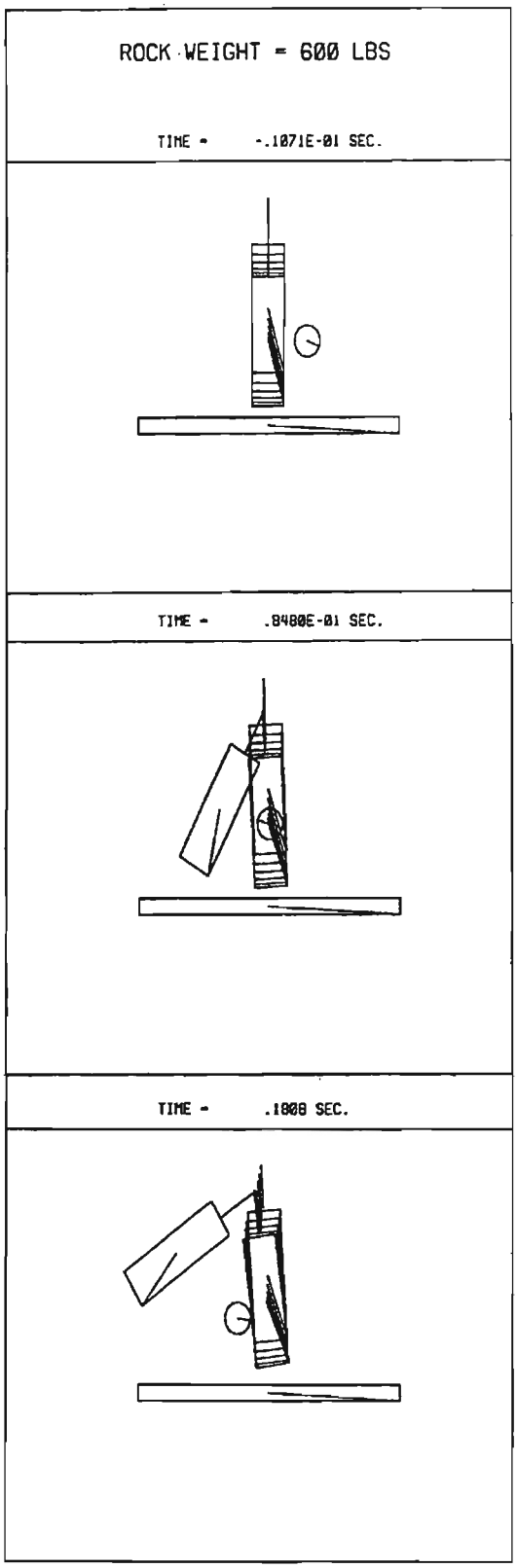

Fig. 13 Impact of 600 LB Rock, without Bottom Cable: Geometry Plot

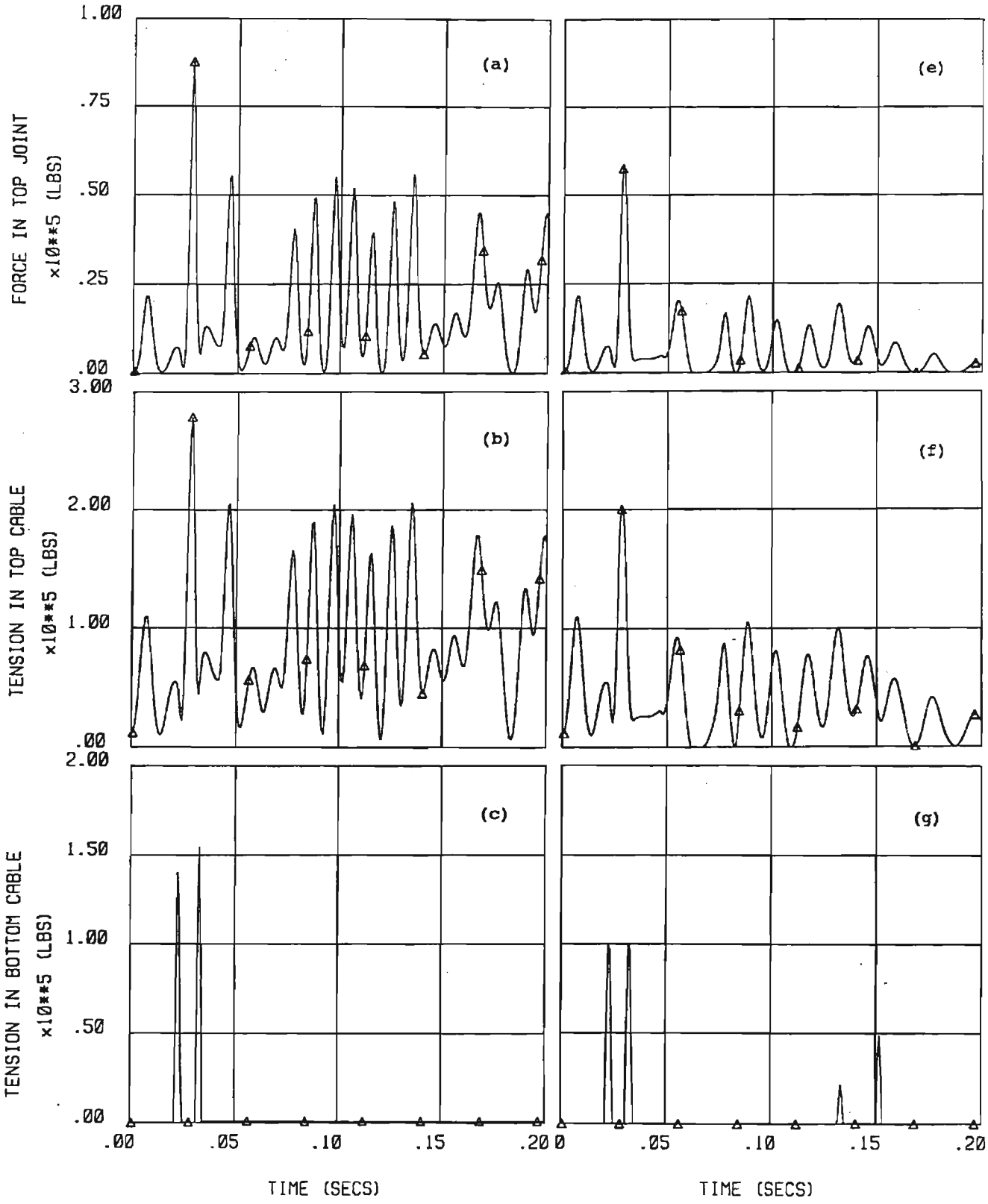

Fig. 14 Impact of 600 LB Rock, with Bottom Cable (Slack = 0.5 FT): (a) to (d) Time History Plots for Elastic Cables, (e) to (i) Time History Plots for Elaso-Plastic Cables

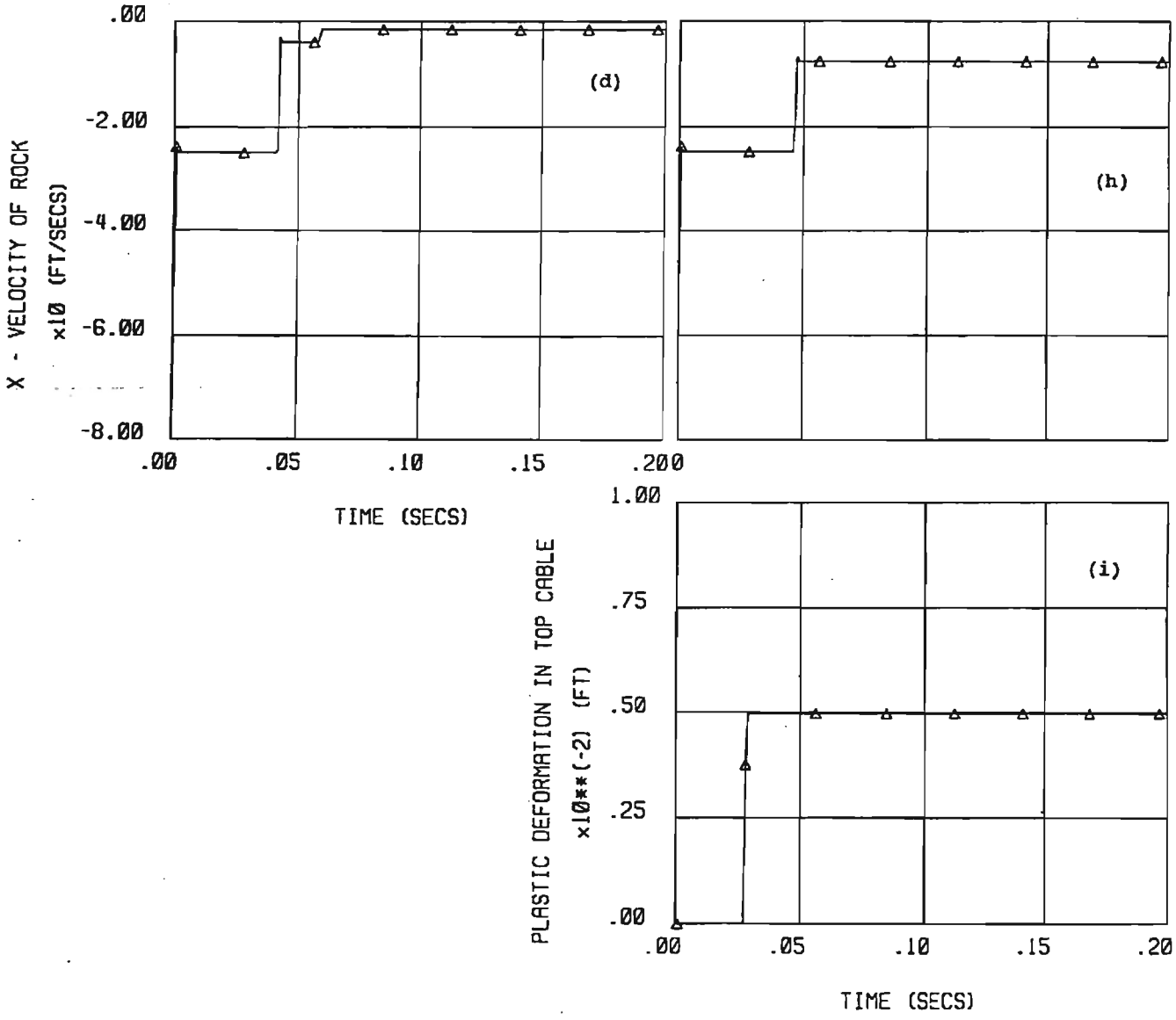
.00
-2.00
-4.00
-6.00
-8.00
X - VELOCITY OF ROCK
×10 (FT/SECS)
.00
.05
.10
.15
.200
TIME (SECS)
(d)
(h)
1.00
.75
.50
.25
.00
PLASTIC DEFORMATION IN TOP CABLE
×10**(-2) (FT)
.00
.05
.10
.15
.20
TIME (SECS)
(i)

Fig. 14 (Cont.)

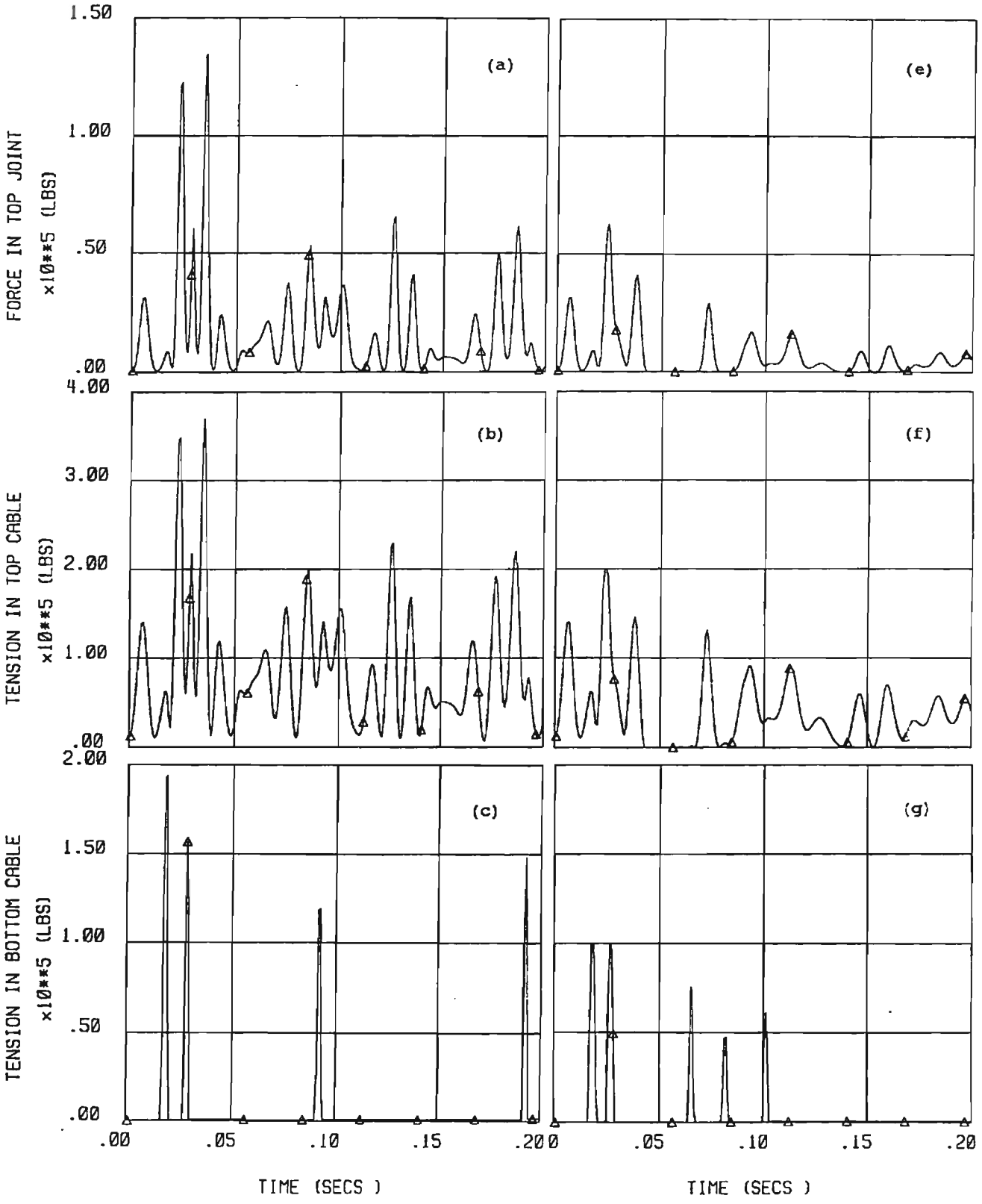

Fig. 15 Impact of 1200 LB Rock, with Bottom Cable (Slack = 0.5 FT): (a) to (d) Time History Plots for Elastic Cables, (e) to (i) Time History Plots for Elasto-Plastic Cables

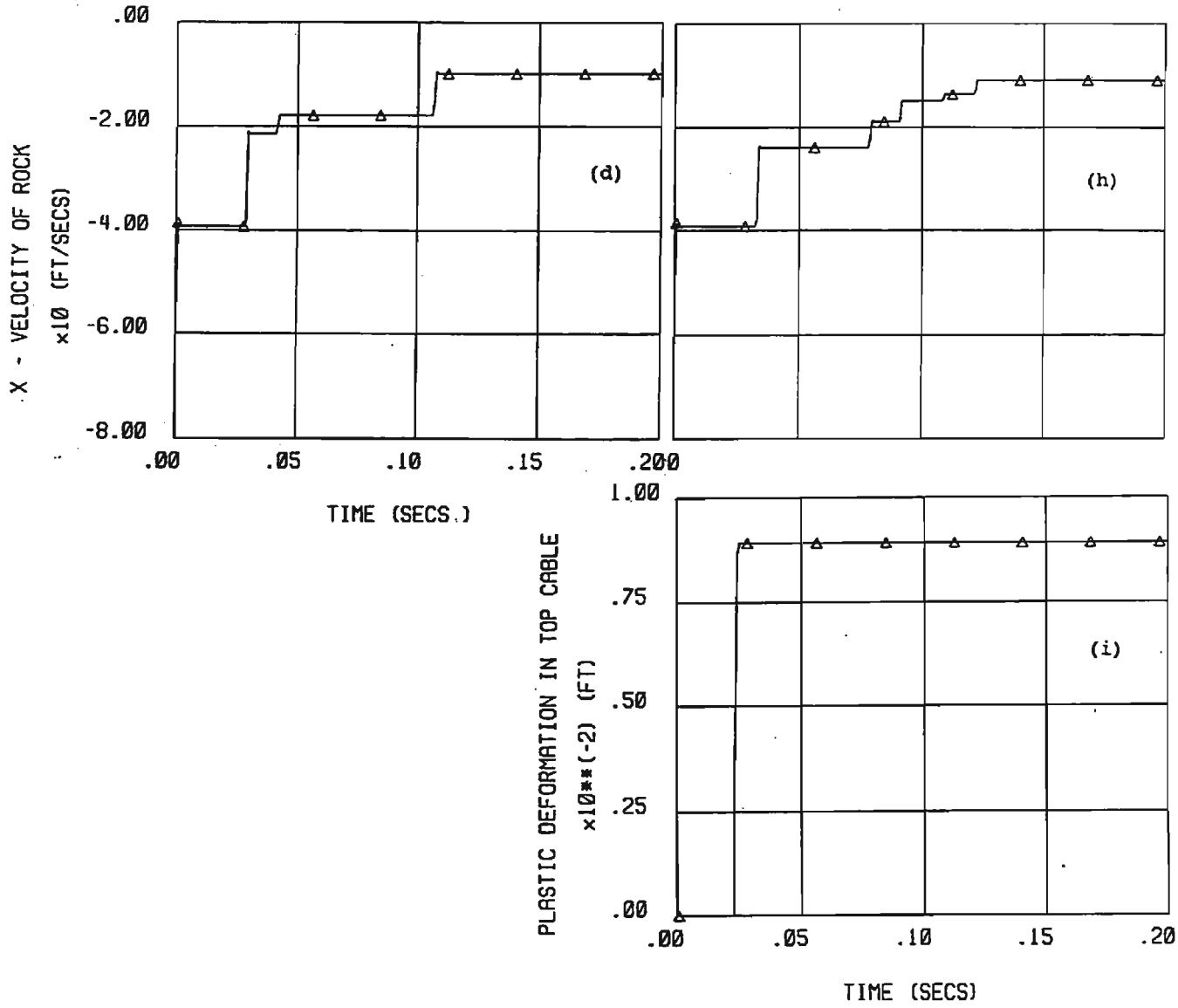
.00
-2.00
-4.00
-6.00
-8.00
X - VELOCITY OF ROCK
x10 (FT/SECS)
(d)
(h)
.00
.05
.10
.15
.200
TIME (SECS.)
1.00
.75
.50
.25
.00
PLASTIC DEFORMATION IN TOP CABLE
x10**(-2) (FT)
(i)
.00
.05
.10
.15
.20
TIME (SECS)

Fig. 15 (Cont.)

APPENDIX I - Modeling of Single and Double Layered Flexible Rockfall Prevention Fences

The following technical paper describes the additional work required to modify the FENCE computer model for the analysis of flexible rockfall prevention fences constructed with two layers of attenuator columns. This publication also illustrates the capability of the FENCE model to simulate multiple rocks impacting a fence structure.

DYNAMIC ANALYSIS OF FLEXIBLE STRUCTURES SUBJECT TO MULTIPLE ROCK-RUBBLE IMPACTS

by

G.G.W. Mustoe
Division of Engineering
Colorado School of Mines
Golden, CO 80401, USA.

Accepted for the Proceedings of the 2nd International Conference on Discrete Element Methods
at
M.I.T., Boston Massachusetts, March. 1993

Abstract

A discrete element model for simulating the dynamic impact response of a highway rockfall prevention barrier system is described. This work is an extension of previous work for modeling single layer fence barriers subject to single rock impacts. The DEM technique employs two-dimensional modeling techniques to develop an efficient algorithm for a three-dimensional nonlinear dynamic structural system. The approach developed herein is suitable for modeling multi-layered flexible barrier systems impacted by single or multiple rocks. The resulting software can be used on microcomputers and is suitable for sensitivity studies and design calculations.

INTRODUCTION

Rockfall prevention highway barrier systems consisting of flexible fence structures are increasingly being used to minimize the risk of rockfall related automobile accidents or road closures. These barriers are placed near highways in mountainous regions wherever there is a significant potential rockfall hazard.

Traditionally, most rockfall prevention highway barrier systems are rigid or semi rigid structures such as fences or walls. Rigid barrier systems are usually constructed from a combination of wood, metal grids and low cost geo-materials which are often available onsite. Because these barriers are designed to completely stop falling rocks they are usually fairly massive structures requiring a large amount of material and significant construction. Alternative rockfall prevention barrier systems are catchment pits or trenches which must be excavated or blasted so that they are deep enough to catch the rocks.

More recently, highway engineers have developed various flexible barrier systems which overcome many of the problems associated with rigid structural barriers or pits. These flexible systems are much smaller and lightweight in construction, and are designed so that minor damage to the barrier can easily be repaired. It should be noted that minor damage should not significantly reduce the effectiveness of the barrier. The basic design concept of these flexible barrier systems is based upon the notion that the flexible barrier does not have to completely stop the falling rock, but just reduce the kinetic energy of the falling rock to an acceptable level after impacting the barrier. The kinetic energy of the rock after impacting the barrier must be such that the rock comes to rest harmlessly in a rolling zone. The concept of reducing the falling rocks kinetic energy is usually termed the principle of rockfall attenuation.

In a flexible barrier system the rock velocity is slowed down by transferring some of its kinetic energy into the flexible barrier system in the form of impact energy losses, inelastic deformational energy and an increase of kinetic energy within the flexible barrier. Typical design considerations for a flexible barrier system are: (i) the accurate prediction of maximum impact forces within the flexible barrier system, and (ii) an estimate of the corresponding kinetic energy loss of the falling rocks.

In order to address these design issues full-scale testing of prototype flexible fences and barrier systems has been performed by the Colorado Department of Highways (CDOH). This experimental work has been successful in determining the overall performance of typical flexible barrier systems, estimating the basic design parameters, and modeling barrier failure mechanisms. The major limitations of the data obtained from this test program are: (i) it is difficult to scale the experimental data for much larger or smaller structures, (ii) limited quantitative information of falling rock kinetic energy losses, and (iii) limited applicability to modifications in the barriers structural design, and (iv) most of the data is qualitative .

Recently, a numerical model based upon a combination of the discrete element methodology and a conventional dynamic structural model has been developed to simulate the dynamic response of a particular flexible rockfall prevention barrier system [1]. This barrier type consists of hanging columnar attenuator masses assembled from used truck tires and rims, threaded onto a steel rod, which are suspended from a horizontal overhead wire cable and connected by a bottom cable. Fig. 1 (a) illustrates a typical two fence layer flexible barrier system. The bottom cable connection is installed to increase the kinetic energy losses of the impacting rocks. This increase occurs because the combined mass of all attenuators are more tightly linked together. It should be noted that any slack in the bottom cable results in a staggered motion of the attenuators. When a rock hits the barrier the hanging columns begin to move in a pendulum-like motion. The sizes of the most likely impacting rocks range between 500 lbs to 1500 lbs. Corresponding impact rock velocities vary between 50 and 70 ft/s. It should be noted that larger impacting rocks that are over 2000 lbs in weight are likely to cause significant fence damage, and exceed the barrier system capacity.

The numerical model described here is a technique that can be used in conjunction with experimental methods to estimate the barrier capacity. For example, the dynamic impact calculations can study the effects of different rock sizes and rock velocities on particular barrier configurations. Barrier response parameters of particular importance include; (i) the forces in the hanger connection and the overhead and bottom cables, and (ii) the decrease in rock velocity due to impact.

The numerical procedure developed is based upon the DEM. This procedure solves the nonlinear coupled dynamic equations of motion for the idealized barrier structure and the impacting rock. The DEM model assumes that the barrier structure can be idealized as a system of connected rigid bodies, and the rock as an impacting rigid body. The dynamic barrier-rock impact conditions are modeled with a penalty formulation and an automatic contact detection algorithm. This numerical procedure utilizes an explicit time stepping scheme to solve the discretized equations of motion, see [1] for further details.

The work presented in this paper is an extension of the analysis technique and associated computer software developed by Mustoe and Huttlemaier [1]. The new developments reported here include: (i) the modeling of rockfall events consisting of multiple rock impacts, and (ii) dynamic analysis of flexible barrier systems consisting of multiple fence structures.

BARRIER DEM MODEL

The rockfall barrier discrete element algorithm includes the following features:

(i) an automatic contact detection scheme which automatically recognizes new contacts as the simulation progresses, and updates the contact topology appropriately,
(ii) a contact force model that determines the forces acting between interacting fence attenuator columns, impacting rocks and connecting fence cables, and
(iii) a time integration scheme to solve the governing equations of motion of the fence attenuator columns and impacting rocks, that allows for finite displacement and rotation.

The modeling aspects and assumptions of the discrete element model, namely the rigid body dynamics of the barrier system and rock, the cable behavior, the rock/attenuator impact interaction model and the numerical integration of the dynamic equations of motion are discussed below:

- The impacting rocks and fence attenuator columns are modeled as three-dimensional rigid spherical and cylindrical bodies respectively, that are confined to move in a planar manner within the x,y plane (see Fig 1 (b)).
- A superquadric representation [2] of the two-dimensional boundaries of the impacting rocks and fence attenuator columns is employed. This kind of geometrical modeling has been used previously by Williams and Pentland [3] in DEM analysis.
- Multiple fence layers within the flexible barrier system interact with each other because of the contact between adjacent attenuator columns in different fence layers. This phenomena occurs because of the planar kinematics of the attenuator columns.
- Multiple interacting rocks are assumed to hit the central localized portion of the barrier that is limited to one or two attenuators in the center of the barrier. This assumption is justified since the diameter of most impacting rocks is less the diameter of the cylindrical attenuator columns.
- The connecting cable segments between neighboring attenuators in the same fence layer are modeled as elastic or elasto-plastic massless elements that only transmit tensile forces.
- Contact forces are generated from contact stiffness and damping elements which act between the central attenuator(s) and the impacting rocks or between adjacent attenuator columns in different fence layers. These forces are determined from the current penetration or overlap distance and the relative velocities of the bodies in contact at the common point of contact. Note, that contact forces between adjacent attenuator columns in the same fence layer are neglected, since they are small compared with the impact force between the central attenuator and the impacting rocks.

BARRIER MODEL EQUATIONS

Equations of Motion

The equations of motion for the i^{th} fence attenuator within a fence layer modeled as a rigid body, assuming planar dynamic motion confined in the x-y plane are given by:

$$m_i \ddot{x}_i = \Sigma F_{xi} \tag{1}$$

$$m_i \ddot{y}_i = \Sigma F_{yi} \tag{2}$$

$$I_i \ddot{\theta}_i = \Sigma M_i \tag{3}$$

for $i = 1,2,...N$, where N_a is the total number of fence attenuators, and N is defined as $N = (N_a + 1)/2$. This definition of N is because of the impacting rock(s) are assumed to hit the central fence attenautor column. See Fig. 1 (c) for details of the attenuator DEM idealization. The corresponding resultant loading terms in equations (1),(2) and (3), are:

$$\Sigma F_{xi} = \overline{T}_{xi} + \overline{B}_{xi} + P_{xi} \tag{4}$$

$$\Sigma F_{yi} = \overline{T}_{yi} + \overline{B}_{yi} + P_{yi} - m_i g \tag{5}$$

$$\Sigma M_i = \overline{B}_{xi}\, b\cos\theta_i + \overline{B}_{yi}\, b\sin\theta_i + \overline{T}_{xi}\, a\cos\theta_i + \overline{T}_{yi}\, a\sin\theta_i + P_{xi}\,\Delta y_i + P_{yi}\,\Delta x_i \qquad (6)$$

where $\overline{T}_{xi}$ and $\overline{T}_{yi}$ are the global x- and y- components of tension forces induced at the top overhead cable connection, $\overline{B}_{xi}$ and $\overline{B}_{yi}$ are the global x- and y- components of tension forces induced at the bottom cable connection, P_{xi} and P_{yi} are the global x- and y- components of the contact forces generated by the rock attenuator impact, and g is the gravitational constant. For the i^{th} attenuator the following parameters are defined: m_i is the mass, I_i is the mass polar moment of inertia with respect to the centroid, x_i and y_i are the global centroidal coordinates, and θ_i is an angular coordinate defining the axial direction of the attenuator. The distances of the top and bottom cable connections with respect to the attenuator centroid are defined by a and b, respectively. The global x- and y- coordinates of the point of contact of the rock with the attenuator measured with respect to the attenuator centroid are defined by Δx_i and Δy_i. Note, that if N is even, the mass and moment of inertia terms in equations (1) through (3), for i=1, are doubled. This modification is required because of the assumed symmetrical impact geometry which implies that the two central attenuators are hit simultaneously.

The corresponding equations of motion for impacting rocks are similar to those developed above for a fence attenuator, and are not repeated for sake of brevity. Note, that the cable force terms in the equations of motion for the rocks are zero.

Cable Attachment Forces

The top and bottom cable attachment segment forces are computed using simple equivalent axial cable stiffness coefficients and determining the current change in cable segment lengths from their original initial segment lengths. It is important to note that the initial tension in the cables must be accounted for in these force calculations. For further details, see Mustoe and Huttlemaier [1]. When modeling the slack in the bottom cables it should be noted that a significant amount of slack cable length must be taken up before any tensile forces are transmitted to the attenuators.

Interaction Force Laws

A simple dynamic contact model is used, since the energy transfer mechanism between the rock and the fence is of primary interest. The normal contact element model is comprised of a linear spring stiffness and viscous damper, connected in parallel, that acts in the contact normal direction at the instantaneous point of contact. Behavior in the contact shear direction is defined by a shear contact element model consisting of a linear spring stiffness and a slider that simulates a simple Coulomb dynamic friction model. Note, that the contact normal and shear directions are defined by the boundary geometry of the body with the smoothest tangent plane at the point of contact. The normal and shear contact element model are active only when the discretized boundaries of the rock and the attenuator penetrate each other.

The normal instantaneous contact force, F_n, is defined by:

$$F_n = \begin{cases} k_n \delta_n + c\dot{\delta}_n & \delta_n \geq 0 \\ 0 & \delta_n < 0 \end{cases} \qquad (7)$$

where, k_n is the normal contact stiffness, c is the normal contact viscous damping coefficient, and δ_n is the normal penetration distance at the point of contact.

The shear instantaneous contact force, F_s, is given by:

$$F_s = \begin{cases} k_s \delta_s & k_s|\delta_s| < \mu |F_n| \text{ and } \delta_n > 0 \\ \mu F_n & k_s|\delta_s| \geq \mu |F_n| \text{ and } \delta_n > 0 \\ 0 & \delta_n < 0 \end{cases} \quad (8)$$

where, k_s is the shear contact stiffness, δ_s is the shear slip distance at the point of contact and μ is the dynamic coefficient of friction between the rock and the attennator.

Note: A suitable value of the normal contact stiffness k_n is specified by the user by limiting the maximum penetration, or overlap, between the surfaces of the impacting two bodies to a predefined value. Typically, this maximum penetration is defined as a small fraction of the average body dimension of the contacting bodies. An estimate of k_n can simply be determined with an approximate energy calculation for the two impacting bodies during an elastic collision. This approximate calculation assumes that the bodies are approximated as two particles of mass m_r and m_f, respectively. Using the above approach an estimate for k_n is given by:

$$k_n \approx \left[m_r m_f / (m_r + m_f) \right] v_{max}^2 / \Delta_{max}^2 \quad (9)$$

where v_{max} and Δ_{max} are the estimated maximum normal relative speed and overlap distance at the contact point respectively during the impact.

Restitution Model

In the discrete element numerical model, the energy loss due to impact is simulated with a viscous damper which acts at the point of impact, P, in the contact normal direction. The normal viscous force in this damper, which is the second term in the normal contact force equation (7), is given by:

$$F_c = c \dot{\delta}_n \quad (10)$$

where $\dot{\delta}_n$ is the normal component of the relative velocity of the fence with respect to the rock at the point of contact, and is defined by:

$$\dot{\delta}_n = (\bar{v}_{Pf} - \bar{v}_{Pr}) \cdot \hat{n} \quad (11)$$

Note, that $\hat{n}$ is the unit outward contact normal direction at the point of impact, P, and $\bar{v}_{Pf}$ and $\bar{v}_{Pf}$ are the velocities of the fence and the rock during the impact, respectively, and c is the normal contact viscous damping coefficient as defined in equation (7).

In a dynamic impact between two bodies, the energy loss can be approximately modeled with a simple restitution model that requires e, the coefficient of restitution, to be known apriori via experimental data. Due to lack of available quantitative data concerning the impact energy losses during a barrier-rock impact situation this simple model is appropriate. However, in order to apply the normal contact force law, equation (7), a relationship between the viscous damping coefficient c, and the coefficient of restitution e, is required. For this purpose, a simple approximate relationship between the viscous damping coefficient, c, and the coefficient of restitution, e, can be derived by assuming that the rock and the attenuator are approximated as two particles of mass m_r and m_f, respectively. This results in the relationship:

$$c = 2\ln(1/e)\left[k_n m_r m_f/(m_r+m_f)\right]^{1/2}\Big/\left[\pi^2+(\ln(1/e))^2\right]^{1/2} \qquad (12)$$

where k_n is the normal contact stiffness at P, the point of impact.

It should be noted that the use of equation (12) is only approximate when applied to a non-central impact between a spherical rock and a cylindrical attenuator. Some numerical experimentation, therefore, is usually required to obtain the precise value of the viscous damping coefficient which corresponds to a specified value of the coefficient of restitution.

Contact Detection Algorithm

The multiple contacts which occur between the rocks and the fence attenuator columns are detected automatically with an algorithm which performs the following functions:
(i) At the beginning of the analysis the problem space is subdivided into a grid of rectangular cells or subregions. The dimensions of these cells is defined to be a function of the average dimension of the bodies within the problem and selected to minimize computational effort.
(ii) Simple geometrical checks are carried out to determine the cell locations for each body in the problem throughout the simulation as the bodies move.
(iii) At every time step local body-to-body contact checking is performed on a cell by cell manner for cells within the problem space. This algorithm is similar to that developed by Preece and Taylor [4], and the method employed by Zhang [5] for modeling particle flow problems.

Explicit Time Stepping Scheme

The time stepping scheme employed in the DEM procedure is the standard explicit central difference method [1], applied to the equations of motions defined by equations (1) through (3). This leads to three sets of generalized velocity and displacement update formulas for the centroidal coordinates of a body. Large motion of the bodies (the fence attenuators and rocks) is simulated with successive incremental updating of the bodies current coordinates.

DEM IMPACT ANALYSES

Model Dimensions and Properties

A full size barrier model is used to study the dynamic response of the barrier system due to impacting rocks. A similar full size prototype barrier system has been built by the Colorado Department of Highways (CDOH). Limited experimental data, which is mainly qualitative, has been obtained from this barrier structure by the CDOH. The dimensions and material properties for these numerical analyses are as follows:

Span of top cable	55 ft	
Sag of top cable	5.5 ft	
Youngs modulus of cable		20,000 ksi
Cross section area of top cable		1.076 in^2
Cross section area of bottom cable		0.25 in^2 (double wrapped)
Fence attenuator height		8 ft
Fence attenuator width		2.5 ft
Rod attachment length		2.5 ft
Fence attenuator unit weight		12.2 lbs/ft^3
Rock diameter		2.5 ft
Rock weight		1200 lbs
Rock impact velocity		53 ft/s^2
Coefficient of restitution		0.4
Maximum estimated contact overlap		0.5 ft

In the present computer model the cable behavior is modeled with a simple linear elastic model. It should be noted that more realistic material models for the cable can be readily inserted into the present algorithm. For example, a constitutive model with time dependent stiffness properties which accounts for cable life [6], could be easily implemented.

Analysis Results

A series of analyses were performed to study the influence of the following design variables: (i) barriers systems consisting of one and two fence layers, (ii) single and multiple rocks impacting the barrier systems, and (iii) barriers with and without a bottom cable. All analyses assumed that the bottom cable segments had a 0.5 ft initial slack length. The maximum estimated contact overlap of 0.5 ft was chosen to approximate the local contact deformation of the fence attenators which are constructed from rubber tires and rims.

Each computer run was performed with a time step length of approximately $\Delta t = 2 \times 10^{-4}$ seconds. The analyses performed here required between 5 and 15 minutes of CPU, on an Intel 80386, 33 MHz CPU microcomputer.

Geometrical snapshots of the barrier geometry and impacting rocks for four different simulations are shown in Figs. 2 and 3. Figs. 2 (a) through (c) illustrate a single rock impacting a single layer fence barrier system with top and bottom cable attachments. Figs. 2 (d) through (f) illustrate a single rock impacting a two layered fence barrier system with top and bottom cable attachments. Figs. 3 (a) through (c) illustrate nine rocks (with a total combined weight of 1200 lbs) impacting a two layered fence barrier system with top and bottom cable attachments. Figs. 3 (d) through (f) illustrate a single rock impacting a two layered fence barrier system with only a top cable attachment.

Comparison of Fig. 2 (a) through (c) and Fig. 2 (d) through (f) shows the following: (i) similar dynamic rock motion during these two impacts, and (ii) the dynamic response of the two layered fence barrier is significantly less than that of the single fence barrier system. The simulations for the two layered fence barrier systems with one and two cable attachments respectively that were subject to a single rock impact illustrate the effect of the bottom cable attachment. The bottom cable stiffens the barrier system and decreases the rock velocity more than a barrier system without a bottom cable (see Figs. 2 (d) through (e), and Figs. 3 (d) through (e)). The effect of multiple or single rocks impacting a barrier system is illustrated in Figs. 2 (d) through (f), and Figs. 3 (a) through (c). The overall response of the barrier system is similar in these two cases.

A comparison of the rock velocities for the above simulations are illustrated in Figure 4. All of the barrier systems with top and bottom cable attachments essentially absorb all the kinetic energy of the impacting

rock (or rocks). The barrier system with only a top cable only reduces the rock velocity from 53 ft/s. to 32 ft/s. Figs. 5 (a) and (b) show the time histories of the dynamic forces generated in the top joint of the central vertical attenuator rod for the four simulations. Fig. 5 (a) shows the effect of the bottom cable in a barrier system on the dynamic loads generated in the top joint. The high peak load at 0.05 seconds in the barrier with two cables is because the 0.5 ft.of initial slack in the bottom cable has been taken up and become taut. Fig. 5 (b) shows that the highest peak force is experienced by the single fence barrier system. This figure also shows that the maximum force generated in the two layered fence barrier impacted by nine rocks is similar in magnitude to the single rock impact simulation. Note the effect of the multiple rock impacts is seen in the smaller peak loads after 0.08 seconds.

CONCLUDING REMARKS

A powerful numerical modeling tool has been developed for the non-linear dynamic impact modeling of a flexible rockfall prevention barrier system. An approximate three-dimensional impact analysis has been performed in an effective manner with a new two-dimensional DEM model. In this model the barrier system and rock kinematics are assumed to be planar, whereas the cable stiffness effects are modeled in a three-dimensional manner. Nonlinear cable effects can be modeled and have been discussed elsewhere [1].

A DEM simulation procedure for modeling flexible barrier systems with multi-layered fence structures subject to single and multiple rock impacts has been developed and demonstrated. This numerical model has been applied to a series of full scale barrier-rock impacts. The numerical results for this series of impact simulations predict the maximum forces generated within the fence cables and the column connections during a rock impact event. Corresponding predictions of post impact rock velocities have also been made. These initial calculations presented here illustrate the ease with which a designer can evaluate the effects of varying different barrier system design parameters on the barrier capacity. It is hoped that further use of this numerical model by the CDOH, in conjunction with additional experimental data, will enable the design engineer to improve upon the current methodology employed in the design of flexible rockfall prevention barrier systems.

ACKNOWLEDGMENTS

The author wishes to acknowledge the financial support of this research work by the Colorado Department of Highways. The authors would also like to thank Robert Barrett, Richard Griffin and Michael McMullen at the CDOH, for their continued interest and helpful discussions during the course of this work.

REFERENCES

1. Mustoe, G.G.W., and Huttelmaier H-P., (1992), "Dynamic Analysis of a Flexible Rockfall Fence Structure by the Discrete Element Method, Microcomputers in Civil Engineering, (accepted for publication, December 1992).

2. Barr, A.H.,(1981) "Superquadrics and Angle-Preserving Transformations", IEEE, Computer Graphics and Applications, Vol. 1, pp. 1-20.

3. Williams J.R., and Pentland A.P., (1989) "Superquadrics and Modal Dynamics for Discrete Elements in Concurrent Design," Proceedings of the 1st U.S. Conf. on Discrete Element Methods", (Mustoe, G.G.W., Henriksen, M. and Huttelmaier, H.P., Eds.), Sponsored by National Science Foundation, Golden, CO., October.

4. Taylor L.M., and Preece D.S., (1989) "Simulation of Blasting Induced Rock Motion Using Spherical Element Models," Proceedings of the 1st U.S. Conf. on Discrete Element Methods", (Mustoe, G.G.W.,

Henriksen, M. and Huttelmaier, H.P., Eds.), Sponsored by National Science Foundation, Golden, CO., October.

5. Zhang, R., (1993), "DEM Simulation of Hydraulic Problems," MSc. Thesis, Engineering Division, Colorado School of Mines

6. Wire Rope Technical Board, (1990) "Wire Rope Users Manual", Third Edition, American Iron and Steel Institute.

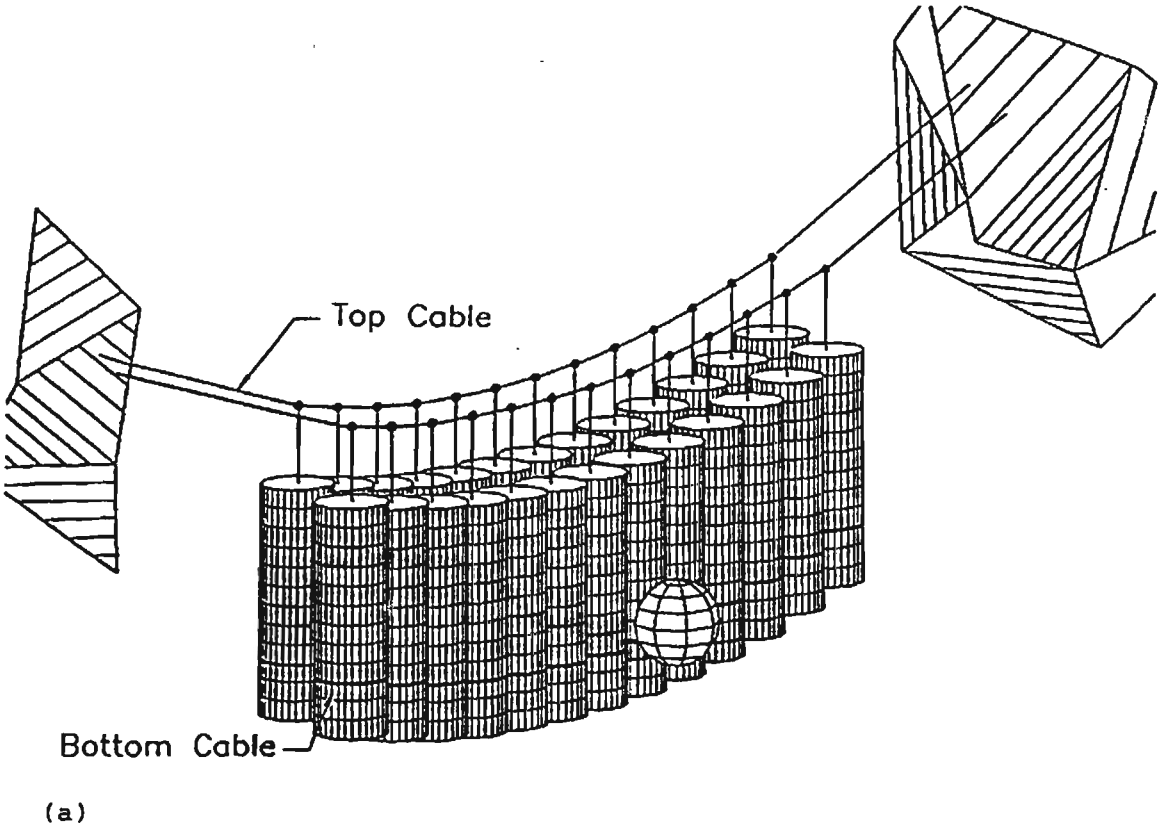

(a)

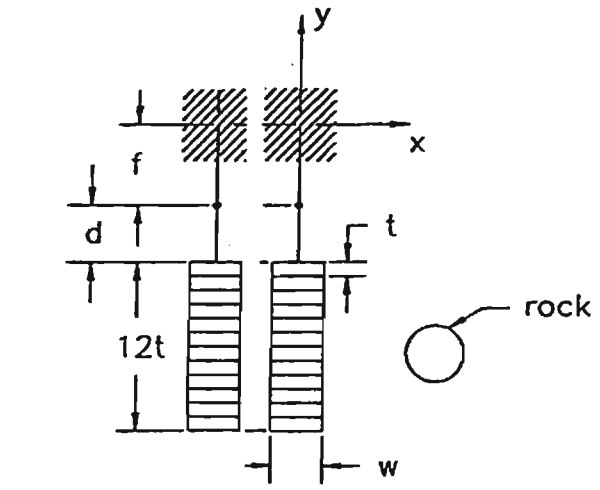

(b)

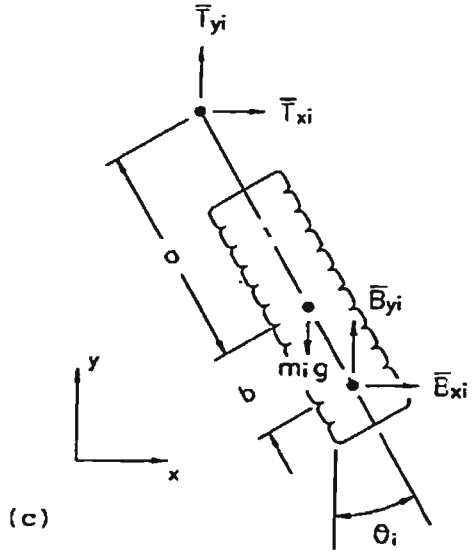

(c)

Fig. 1 A Typical Flexible Rockfall Barrier System. (a) Three-dimensional View of a Two Layered Fence Barrier, (b) Side View of a Two Layered Fence Barrier, (c) DEM Idealization of a Fence Attenuator Column.

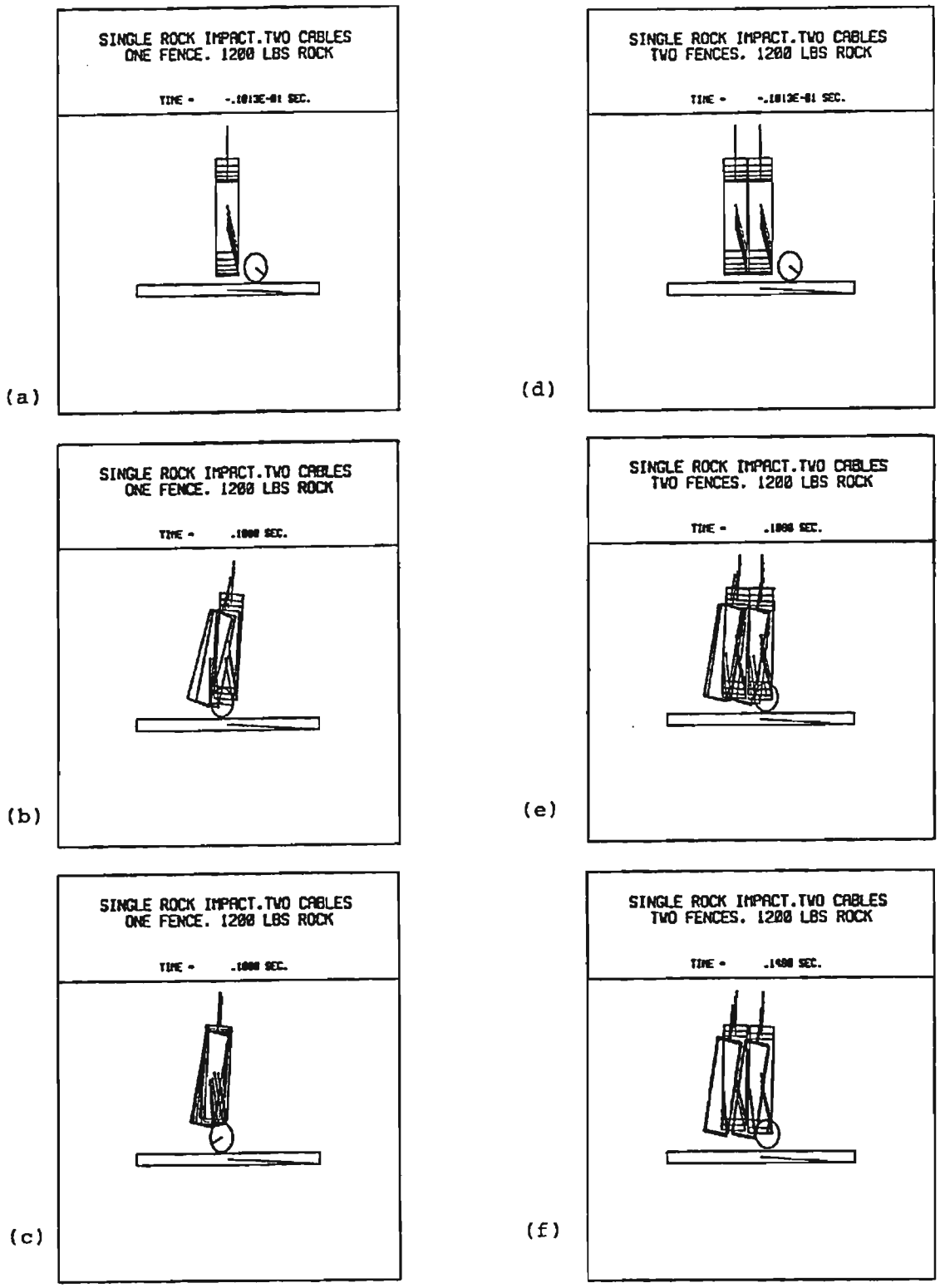

Fig. 2 Geometrical Snapshots of a Barrier-Rock Impact Simulation, Figs. 2 (a),(b) and (c) are for a Single Layered Fence Barrier, Figs. 2 (d),(e) and (f) are for a Two Layered Fence Barrier

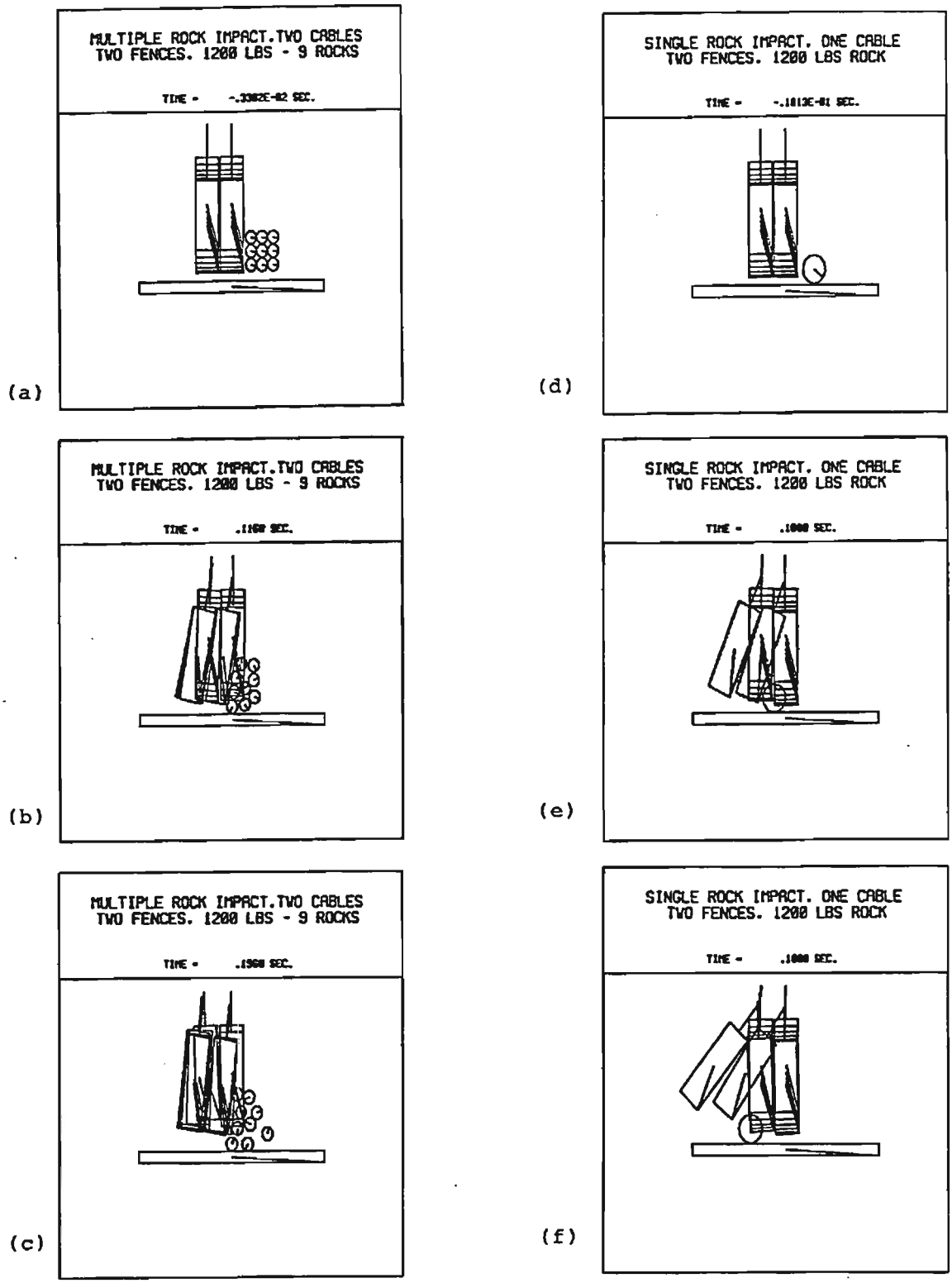

Fig. 3 Geometrical Snapshots of a Barrier-Rock Impact Simulation, Figs. 3 (a),(b) and (c) are for a Two Layered Fence Barrier subject to a Multiple Rock Impact, Figs. 3 (d),(e) and (f) are for a Two Layered Fence Barrier with a Top Cable Attachment only.

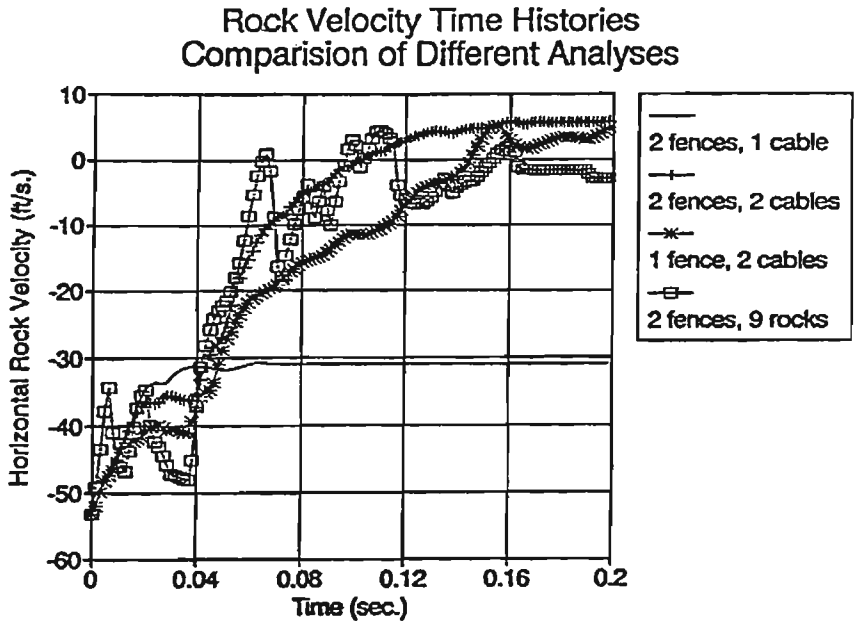

Fig. 4 Rock Velocity Time Histories for Different Barrier-Rock Impact Simulations

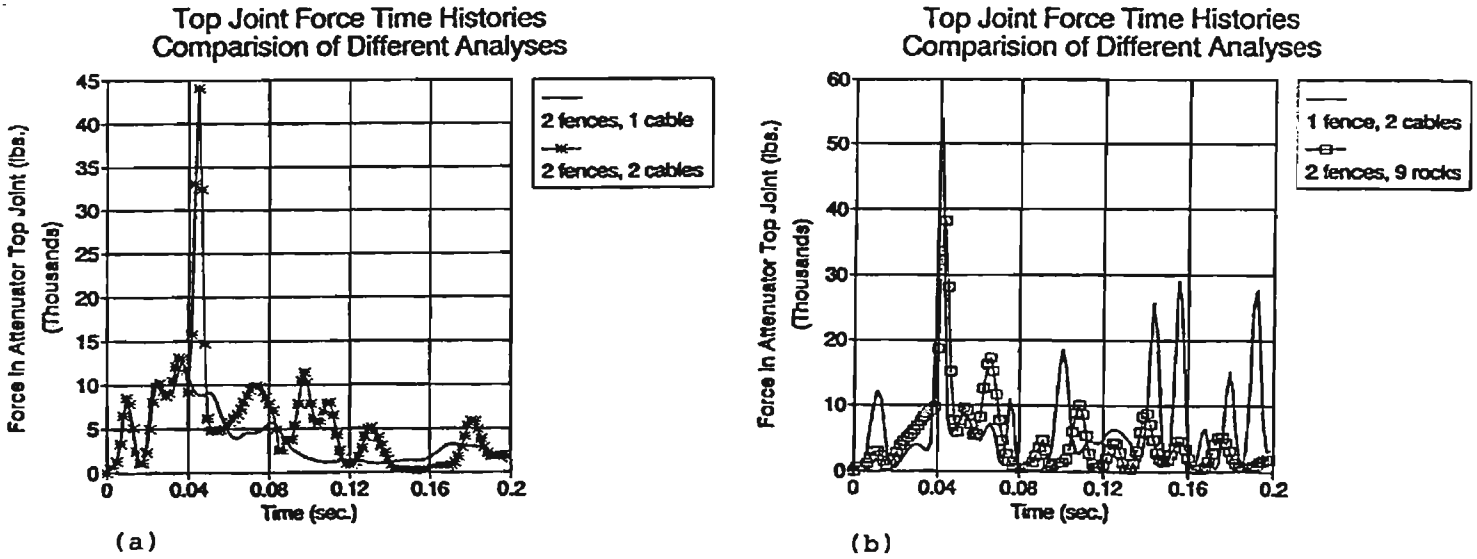

Fig. 5 Dynamic Forces generated in the Top Joint of the Central Vertical Attenuator Rod. (a) Simulations of One and Two Layered Fence Barrier Systems with Bottom Cable Attachments, (b) Simulations of Two Layered Fence Barrier Systems subject to a Multiple Rock Impact, and with a Top Cable Attachment only.

APPENDIX II - Computer Instructions and Users Manual for FENCE

Computer Instructions and Users Manual for FENCE

Abstract

This manual is a detailed guide for the FENCE discrete element computer software package. It also describes the necessary steps that an engineer must undertake to perform a dynamic impact rock-fence analysis using the FENCE discrete element computer software package.

Contents

II.1 Introduction

FENCE is a special purpose computer program based on the Discrete Element Method (DEM) written for the Colorado Department of Highways (CDOH). The program performs rock impact calculations for a specific type of flexible rockfall fence type, The fence model used for this analysis of a series of attenuators suspended from a steel cable and is based on a prototype developed by CDOH. The theoretical foundation of the discrete element formulation for this specific application is discussed in previous chapters of this report. The fence model description is also included earlier in this report, in addition, fence input parameters are discussed below. This Appendix is intended as a guideline for the program user and includes: (i) an overview of the computer software including the different executable modules, and the associated input, output and graphics data files, (ii) the general strategy required to perform an impact analysis using FENCE, (iii) a detailed description of the parameters within a FENCE input file, and (iv) an example that guides the user through the analysis procedure.

II.2 Program Overview and File Definitions

The DEM dynamic fence-rock analysis software FENCE consists of three major modules: (i) the computational DEM executable module (FENCE) that performs the dynamic impact calculation, (ii) the interactive graphics geometrical snapshot and animation executable module (GPLOT), and (iii) the interactive graphics executable module for time history results (HPLOT).

For the DEM computational module, FENCE, the input data contains the following parameters:

(i) fence and rock geometry and mass properties,
(ii) material model and properties for the fence cables,
(iii) impact and restitution parameters between the fence and the rock,
(iv) the initial rock velocity prior to impact, and
(v) control parameters which describe the type and time interval sampling interval for saving computed results.

This input data is contained in a data file with a user-specified name appended with the extension .DAT.

The computed results are written to three different output data files with a user-specified name appended with the extensions .OUT, .HST, and .GEO, respectively. These output data files are called the printout file, the time history file, and the geometry file, respectively.

The printout file is used directly to verify the input data and for checking purposes by the user. The time history and the geometry results data files are input data for the graphical post-processing modules HPLOT and GPLOT, respectively.

The HPLOT graphics module interactively displays time history plots and produces postscript graphics output. Typical time history data plots include; (i) centroidal kinematics quantities such as position and velocity components for the rock and the attenuator columns, and (ii) forces in the overhead and bottom cable segments, and the attenuator hanger connections.

The GPLOT graphics module is used to display the following geometrical data for the fence-rock system; (i) single snapshots of the fence-rock geometry at prescribed times during the impact, or (ii) animation of the fence-rock motion throughout the impact. Postscript graphics output of the single geometry snapshots can also be produced by GPLOT.

In the example illustrated in Figure II.1 the user-specified name for the input data file is fname1, and the user-specified name for the output data files is fname2.

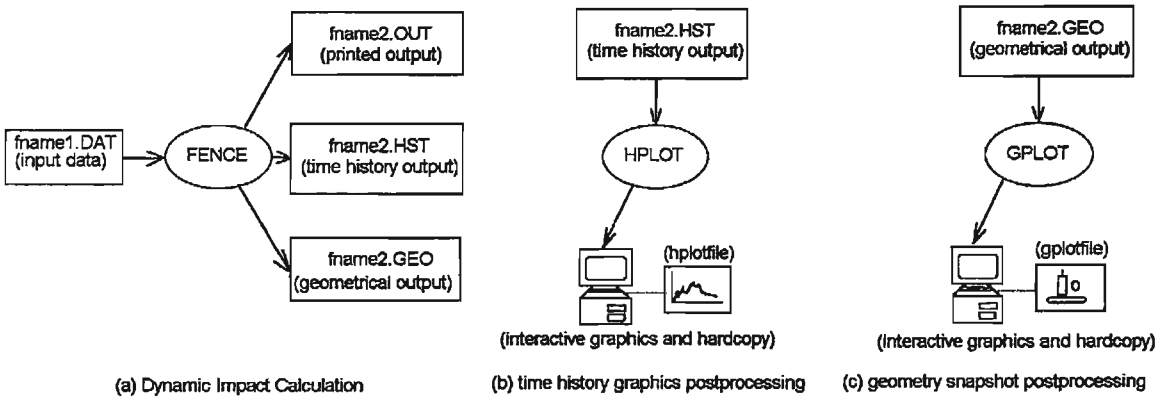

Figure II.1 Execution Sequence of FENCE Computer Software:

The data file definitions for the above figure are as follows:

(i) fname1.DAT: Input File, where fname1 is a user defined name,
(ii) fname2.OUT: Output File in ASCII format, where fname2 is a user defined name,
(iii) fname2.HST: Time History Plot File in binary format,
(iv) fname2.GEO: Geometry Plot File in binary format,
(v) hplotfile: 'Postscript' File for printer plot of time history results,
and (vi) gplotfile: 'Postscript' File for printer plot of geometry snapshot results.

II.3 Modeling Strategy with FENCE Software

When performing a rock-fence impact analysis the following strategy is recommended:

(i) Gather the relevant design data about the fence structure and the impact conditions. This data includes: (a) the geometrical configuration of the fence and attenuator masses, and (b) the shape and mass of the impacting rock and its initial impact position relative to the fence and the impact velocity.

(ii) Make a simple sketch of the side view (x,y plane) of the impact geometry. This will be used to define the input geometry data.

(iii) Decide what results are required from the analysis. This includes the following: (a) how much printed output is needed (This can be voluminous, so be careful.), (b) which elements (fence, rock and attenuators) must be flagged for results output purposes, (c) what time history information is needed, and (d) what geometrical snapshot information is needed.

(iii) Generate an input data file with a user defined name with an extension .DAT.

(iv) Perform an initial test run to verify the input data. This can accomplished by running the analysis for one time step only. Check the input data by reviewing the .OUT file for the following likely errors: (a) incorrect geometry of the fence, or initial position of the impacting rock, (b) check fence and rock masses and initial rock velocity, (c) check the total span and initial sag of the top overhead cable, (d) check the horizontal spacing between attenuator columns, (e) check maximum specified overlaps between rocks and attenuators elements and restitution coefficient. Verify the problem geometry by viewing the initial configuration with the GPLOT graphics module.

(v) Re-run problem for approximately 200 time steps to check the initial impact kinematics, such as the initial speed and direction of the impacting rock. Check the initial impact parameters graphically with GPLOT. If there is a problem with the impact parameters change the initial impact parameters in the .DAT input file. If the data verifies determine the number of time steps required for a complete simulation, change the .DAT input file, and make the final run for the complete impact simulation.

NOTE: There are number of example data files provided with the DEM computer software. Therefore, many of the above steps can be performed quickly by copying an existing data file and modifying it accordingly for a particular rock-fence impact analysis.

II.3.1 Details of the Fence-Rock Geometrical Configuration Definitions required by FENCE Input Data

In a typical fence-rock impact analysis only the geometry of three bodies is required. These bodies (or elements) are usually: (i) the ground or base element, (ii) the rock

element, and (iii) the central attenuator element. Figure II.2. shows the general situation for a single rock impacting a fence. For the problem defined in Figure II.2 it should be noted that the geometry for elements 1 through 3 has to be defined. The geometry of elements 4 through 7 is generated automatically. Note that elements 4 through 6 are slave attenuator elements, and element 7 is a dummy fixed attenuator element .

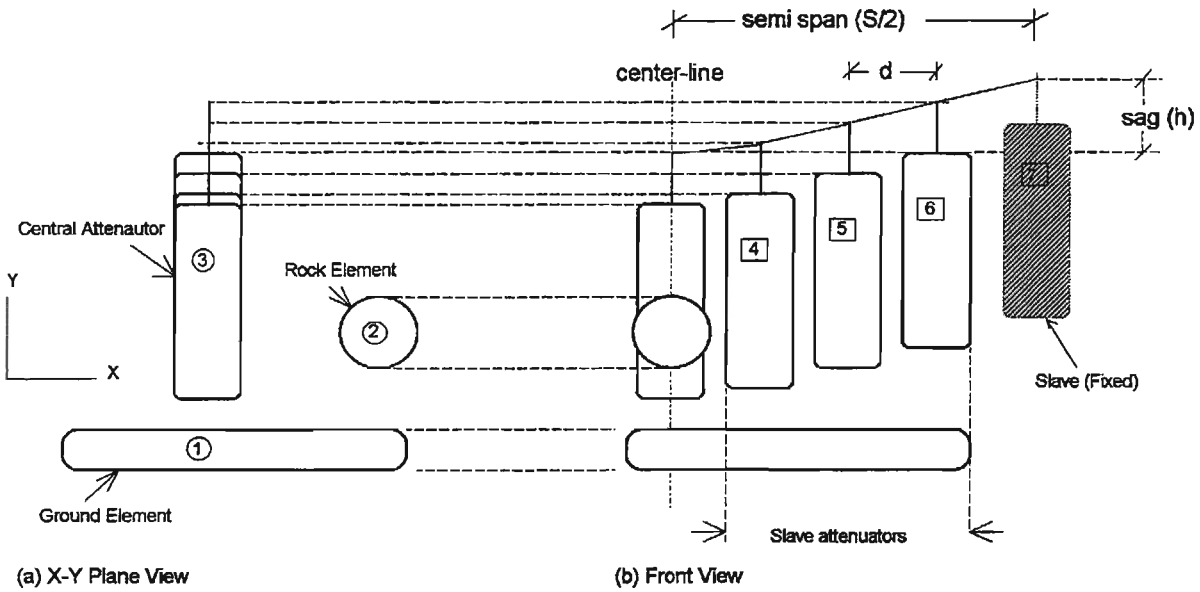

Figure II.2 Typical Geometrical Configuration for a Rock - Single Layer Fence Impact Analysis

The following points should be noted in defining the geometry for a problem:

(i) the elements representing the ground, the rock and the central attenuator should be defined in this order. For example, the ground is element 1, the rock is element 2 and the central attenuator is element number 3. Note that if multiple rocks are defined they must be defined sequentially. In a three rock impact analysis, the ground is element 1, the rocks are elements 2 through 4, and the central attenuator is element number 5.

(ii) the total number of attenuators, not accounting for symmetry must be defined in the input data. For the problem defined in Figure 2, the total number of attenuators is 7. This number is computed from the central attenuator and three slave attenuators on both sides. Note an additional attenuator element is used for fixity purposes in the FENCE model. In this example it is element 7. This element, however, is not defined by the user.

(iii) the total span, S, the sag height h, and the spacing between the centers of adjacent attenuators d, must be defined

(iv) the i^{th} cable segment is defined as the segment on the immediate right of attenuator element i.

(v) an example of the element numbering for a two layered fence barrier is shown in Figure II.3.

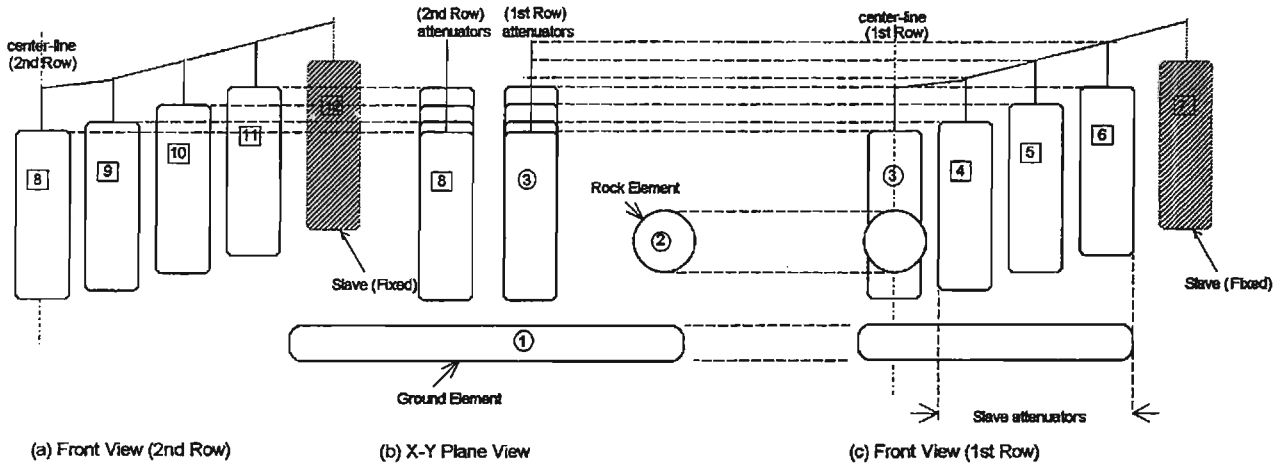

Figure II.3 Typical Geometrical Configuration for a Rock - Double Layer Fence Impact Analysis

II.3.2 Boundary Geometry Definition of the Ground, Attenuators and Rocks with Superquadrics

In the two-dimensional discrete element FENCE model the rigid bodies that represent the attenuators, the ground surface and the rock(s) are idealized with a superquadric geometrical description. For further details of superquadric functions, see Barr (1981).

For the i^{th} body the following parameters are defined: m_i is the mass, I_i is the mass polar moment of inertia with respect to the centroid, X_i and Y_i are the global centroidal coordinates, and θ_i is an angular coordinate defining the direction of the local x-direction defined by the principal axis of the body with respect to the global X-direction (see Figure II.4). The parameters that define the shape of the body are a_i, b_i, and n_i and are defined as the semi-lengths of superquadric in the local centroidal x- and y- directions, and the real exponent which specifies the roundness of the superquadric respectively.

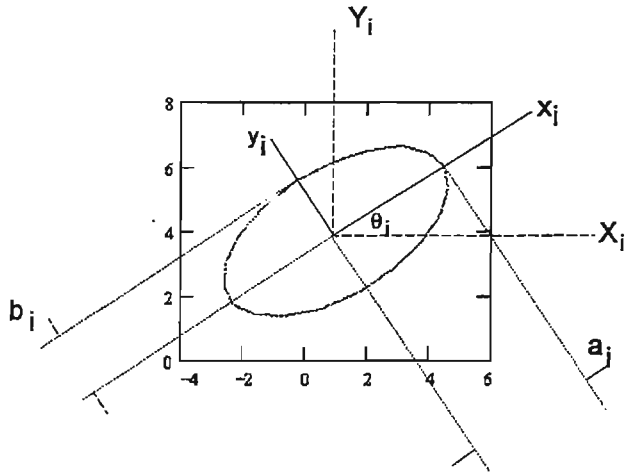

Figure II.4 Definition of Local and Global Superquadric Geometry

II.4 Description of the FENCE Input Data File

This section describes the input parameters and the required format for the input file with an extension .DAT. The READ statements described below are contained in the input source file INPUT.FOR.

READ(*,'(A)') **flinp**

flinp = screen prompt for input data file (e.g. fname1)

READ(*,'(A)') **flout**

flout = screen prompt for output files (e.g. fname2)

READ(iin,'(a)') **ptitle**

ptitle = title line for input data (1st line in fname1.DAT)

READ(iin,*) **fact_dt,niter,nprint,nhisto,f_penet**

fact_dt = factor of critical time step length
niter = number of time steps (iterations)
nprint = number of time step intervals between writing results onto .OUT and .GEO files
nhisto = number of time step intervals between writing results to .HST file
f_penet = minimum penetration between rock and attenuator during impact defined as fraction of the bounding dimensions of bodies.

NOTE: This can be overidden by using an explicit definition of maximum penetration between attenuator and rock elements and attenuator and attenuator elements. See READ(iin,*) rf_overlap, ...

READ(iin,*) **nel,igrav,grav**

nel = number of elements (e.g., for slope, attenuators and rock (or rocks))
NOTE: usually nel = 3
igrav = 1 ... gravity acts in positive y-direction
igrav =-1 ... gravity acts in negative y-direction
grav = gravitational constant

READ(iin,*) **elstore**

elstore = number of elements tagged for recording time history results

READ(iin,*) **(elnos(i),i=1,elstore)**

elnos = array of element I.D's tagged for recording time history results

READ(iin,*) **totvar**

totvar = no. of variables to be stored (max. =6)

READ(iin,*) **(variab(i),i=1,hvmax)**

variab = list of time history variable codes to be recorded for elements in elnos()

NOTE: these integer codes are defined in global.par source file and printed in the .OUT file.

*** beginning of element loop, i = 1,nel

READ(iin,*) **type,shape,points**

type = (rock=0, attenuator=1)
shape = (sphere or)
(ellipsoid (rock) = 0)
(rectang. block (rock) = 1)
(cylinder (attenuator) = 2)

points = number of nodal points on superquadric

READ(iin,*) **xlen,ylen,power,rho,barlen**

xlen = length in x-dir. (a_i)
ylen = length in y-dir. (b_i)
power = power of superquad (n_i)
rho = mass density
barlen = attachment length (attenuator only)

Note: See Figure II.4 for superquadric geometry definitions

READ(iin,*) **xcent,ycent,theta,vx,vy,omega,fx,fy,mz**

initial global geometrical and dynamic centroidal conditions for an element:

xcent = x-coordinate
ycent = y-coordinate
theta = rotation
vx = x-velocity
vy = y-velocity
omega = angular velocity
fx = force in x-direction
fy = force in x-direction
mz = moment

READ(iin,*) **bc(1),bc(2),bc(3),xl_fix,yl_fix**

bc(i) = centroidal fixities
bc(i) = 1 .. fixed
bc(i) = 0 .. free
bc(1) = x-direction
bc(2) = y-direction
bc(3) = rotational

*** end of element loop

READ(iin,*)**span,sag,dcol,young,y_top,y_bot,nocab,**
ncol,ecoeff,area_top,area_bot,frict,slack,brek_top,
brek_bot

Definition of fence layer parameters:

span = Horizontal cable span
sag = Vertical cable sag
dcol = Horizontal distance between columns
young = Youngs modulus of cable
y_top = y-coordinate of top cable connection
y_bot = y-coordinate of bottom cable connection
nocab = No. of top/bottom connections on attenuator
ncol = No. of tire attenuator columns in a fence layer
ecoeff = coefficient of restitution
area_top = x-section area of top cable
area_bot = x-section area of bottom cable
frict = coefficient of friction
slack = slack in between bottom connections
brek_top = top cable breaking strength
brek_bot = bottom cable breaking strength

READ(iin,*) no_fence, sp_fence

Multiple fence layer parameters:

no_fence = number of fence layers
sp_fence = center to center spacing between the two fence layer

READ(iin,*) rf_overlap, ff_overlap

Definition of maximum penetration between attenuator and rock elements and attenuator and attenuator elements in different fence layers:

rf_overlap = approximate maximum penetration between attenuator and rock
ff_overlap = approximate maximum penetration between attenuator and attenuator in different layers

*** End of Input Data file ***

II.5 Example Analysis Datafiles and Results

II.5.1 Sample Input Datafile

The following data set is for a double layer fence structure being impacted by a single rock. This data set is called sample2.DAT on the diskette supplied with FENCE.

Data	Optional Comments
DOUBLE LAYER FENCE	ROCK WEIGHT = 1200 LBS
0.0 3000 60 30 0.05	fact_dt,niter,nprint,nhisto,fact_penet
3 -1 32.18	nel, igrav, grav
5	elstore
2,3,4,5,6	(elnos(i),i=1,elstore)
8	totvar
51 52 48 6 7 8 35 36 0	(variab(i),i=1,hvmax)
0.0 1.0 2.0	type,shape,points - SLOPE ELEMENT
10.0 0.5 0.0 0.1 0.5	xlen,ylen,power,rho,barlen
0.0 -5.0 0.0 0.0 0.0 0.0 0. 0. 0.	xc,yc,th,vx,vy,oma,fx,fy,mz
1.0 1.0 1.0 0. 0.	bc(1),bc(2),bc(3),xfix,yfix
0.0 0.0 4.0	type,shape,points - ROCK
1.201 1.201 0.0 5.13 0.0	xlen,ylen,power,rho,barlen
2.451 0.0 0.0 -65. 0.0 34. 0. 0. 0.	xc,yc,th,vx,vy,oma,fx,fy,mz
0.0 0.0 0.0 0. 0.	bc(1),bc(2),bc(3),xfix,yfix
1.0 2.0 2.0	type,shape,points - FENCE attenuator
1.25 4.0 0.0 0.76 2.67	xlen,ylen,power,rho,barlen
0.0 0.0 0.0 0.0 0.0 0.0 0. 0. 0.	xc,yc,th,vx,vy,oma,fx,fy,mz
0.0 0.0 0.0 0. 0.	bc(1),bc(2),bc(3),xfix,yfix
55.0 5.5 2.5 2.0e7 6.67 -4.0 2 13 0.4 1.076 0.25 0.0 0.5 1e8 1e8	
2, 2.6	- no. fences, spacing between fences
0.6, 0.5	- max. rock and fence overlaps
span,sag,dcol,e,y_t,y_b,nocab,ncol,ecoeff,a_t,a_b,frict,slack,brek_top,brek_bot	

***** End of DATA *****

II.5.2 Sample Output Datafile

The following is selected printed output from sample2.OUT that was produced from executing FENCE with the data set sample2.DAT. This output data set is on the diskette supplied with FENCE.

DOUBLE LAYER FENCE ROCK WEIGHT = 1200 LBS

factor of critical time step = .000E+00
total no. of time steps = 3000
time steps per printout = 60
history time steps = 30

```
 no. of discrete elements       =    3
 igrav ( =1 for positive y-dir.) =   -1
 gravity                        =   .3218E+02


no. of elements for time history records =   5

element history array:

  2   3   4   5   6

no. of variables to be stored (max. 8)  =   8

list of variables to be stored:
(see pointers defined in global.par)

  51   52   48   6   7   8   35   36

 Properties for element no.:   1
 Type  ( rock=0, fence=1 )     =    0
 Shape                         =    1
  ( sphere or                  )
  ( ellipsoid (rock)     = 0)
  ( rectang. block (rock) = 1)
  ( cylinder (fence)     = 2)
Number of points on superquad  =    2
Length in x-dir. (large radius)=   .100E+02
Length in y-dir. (short radius)=   .500E+00
Power of superquad             =   .000E+00
Mass density                   =   .100E+00
Attachment length (fence only) =   .500E+00

Properties for element no.:   2
Type  ( rock=0, fence=1 )     =    0
Shape                         =    0
  ( sphere or                  )
  ( ellipsoid (rock)     = 0)
  ( rectang. block (rock) = 1)
  ( cylinder (fence)     = 2)
Number of points on superquad  =    4
Length in x-dir. (large radius)=   .120E+01
Length in y-dir. (short radius)=   .120E+01
Power of superquad             =   .000E+00
Mass density                   =   .513E+01
Attachment length (fence only) =   .000E+00

Properties for element no.:   3
Type  ( rock=0, fence=1 )     =    1
Shape                         =    2
  ( sphere or                  )
  ( ellipsoid (rock)     = 0)
  ( rectang. block (rock) = 1)
  ( cylinder (fence)     = 2)
Number of points on superquad  =    2
```

Length in x-dir. (large radius)= .125E+01
Length in y-dir. (short radius)= .400E+01
Power of superquad = .000E+00
Mass density = .760E+00
Attachment length (fence only) = .267E+01

Element initial conditions

el.	x-loc	y-loc	theta	vx	vy	ang-v	fx	fy	mz
1	.000E+00	-.500E+01	.000E+00	.000E+00	.000E+00	.000E+00	.000E+00	.000E+00	.000E+00
2	.245E+01	.000E+00	.000E+00	-.650E+02	.000E+00	.340E+02	.000E+00	.000E+00	.000E+00
3	.000E+00	.000E+00	.000E+00	.000E+00	.000E+00	.000E+00	.000E+00	.000E+00	.000E+00

Element fixities

el.	fix-x	fix-y	fix-r	x_local	y_local
1	1	1	1	.000E+00	.000E+00
2	0	0	0	.000E+00	.000E+00
3	0	0	0	.000E+00	.000E+00

Description of Parameter Names in Element Data Structure

I.D number	Description
1	SMALLEST POINTER
2	ELEMENT SHAPE(E.G. SPHERICAL)
3	X - LOCATION OF ELEMENT CENTROID
4	Y - LOCATION OF ELEMENT CENTROID
5	ELEMENT GLOBAL ROTATION - THETA
6	X - VELOCITY OF ELEMENT CENTROID
7	Y - VELOCITY OF ELEMENT CENTROID
8	ANGULAR VELOCITY OF ELEMENT - OMEGA
9	ELEMENT LENGTH X-DIR.
10	ELEMENT LENGTH Y-DIR.
11	POWER OF SUPERQUAD
12	NUMBER OF NODAL POINTS ON SUPERQUAD
13	ATTACHMENT LENGTH (FENCE ONLY) = 0.0 FOR
14	ELEMENT DENSITY
15	ELEMENT MASS
16	ELEMENT MASS MOMENT OF INERTIA
17	EXTERNAL CENTROIDAL FORCE X-DIR.
18	EXTERNAL CENTROIDAL FORCE Y-DIR.
19	EXTERNAL CENTROIDAL MOMENT
20	CENTROIDAL BOUNDARY CONSTRAINT, X-DIR.
21	CENTROIDAL BOUNDARY CONSTRAINT, Y-DIR.
22	CENTROIDAL BOUNDARY CONSTRAINT, ROTATION
23	TOTAL APPLIED ELEMENT LOAD, X-DIR.
24	TOTAL APPLIED ELEMENT LOAD, Y-DIR.
25	TOTAL APPLIED ELEMENT LOAD, ROTATION
26	OLD ELEMENT VELOCITY AT CENTROID X-DIR.
27	OLD ELEMENT VELOCITY AT CENTROID Y-DIR.
28	OLD ELEMENT VELOCITY AT CENTROID ROT.
29	NORMAL CONTACT STIFFNESS
30	SHEAR CONTACT STIFFNESS
31	MASS DAMPING FOR TRANSLATION
32	MASS DAMPING FOR ROTATION
33	LOCAL X-COORDINATE OF A FIXED PT. ON ELE
34	LOCAL Y-COORDINATE OF A FIXED PT. ON ELE

35 ELEMENT KINETIC ENERGY (TRANSLATIONAL)
36 ELEMENT KINETIC ENERGY (ROTATIONAL)
37 ELEMENT KINETIC ENERGY (TOTAL)
38 ELEMENT GRAVITATIONAL ENERGY
39 NODAL SPRING ENERGY (AXIAL)
40 NODAL SPRING ENERGY (SHEAR)
41 NODAL SPRING ENERGY (BENDING)
42 INCREMENTAL SPRING DISPLACEMENT (AXIAL)
43 INCREMENTAL SPRING DISPLACEMENT (SHEAR)
44 INCREMENTAL SPRING ROTATION
45 ELEMENT POTENTIAL ENERGY (GRAVIT. & SPRI
46 TOP CABLE LENGTH
47 BOTTOM CABLE LENGTH
48 TENSION IN TOP CABLE
49 X-COMPONENT OF TENSION IN TOP CABLE
50 Y-COMPONENT OF TENSION IN TOP CABLE
51 FORCE IN TOP JOINT OF ATTENUATOR
52 TENSION IN BOTTOM CABLE
53 X-COMPONENT OF TENSION IN BOTTOM CABLE
54 Y-COMPONENT OF TENSION IN BOTTOM CABLE
55 STIFFNESS OF TOP CABLE
56 STIFFNESS OF BOTTOM CABLE
57 INITIAL LENGTH OF BOTTOM CABLE
58 BREAKING STRENGTH OF TOP CABLE
59 BREAKING STRENGTH OF BOTTOM CABLE
60 TOP CABLE PLASTIC DEFORMATION (FT)
61 LARGEST POINTER (CHECK WITH NPRMAX !)

Fence Support Data Parameters
Horizontal cable span = 55.0
Vertical cable sag = 5.50
Horizontal distance between columns = 2.50
Youngs modulus of cable = .200E+08
y-coordinate of top cable connection = 6.67
y-coordinate of bottom cable connection = -4.00
No. of top/bottom connections on fence = 2
No. of tire columns in fence layer = 13
coefficient of restitution = .400
x-section area of top cable = 1.08
x-section area of bottom cable = .250
coefficient of friction = .000
slack in between bottom connections = .500
top cable breaking strength = .100E+09
bottom cable breaking strength = .100E+09

No. of fence layers = 2
gap between fence layers = 2.60

Maximum overlap (rock/fence) = .6000E+00
Maximum overlap (fence/fence) = .5000E+00

Element I.Ds of attenuators in fence layer: 1
I.D nos. = 3 4 5 6 7 8 9

Element I.Ds of attenuators in fence layer: 2
I.D nos. = 11 12 13 14 15 16 17

element	mass	m.o.i.
1	.4000E+02	.1337E+04
2	.3723E+02	.2148E+02
3	.2985E+02	.1708E+03
4	.2985E+02	.1708E+03
5	.2985E+02	.1708E+03
6	.2985E+02	.1708E+03
7	.2985E+02	.1708E+03
8	.2985E+02	.1708E+03
9	.2985E+02	.1708E+03
10	.2985E+02	.1708E+03
11	.2985E+02	.1708E+03
12	.2985E+02	.1708E+03
13	.2985E+02	.1708E+03
14	.2985E+02	.1708E+03
15	.2985E+02	.1708E+03
16	.2985E+02	.1708E+03
17	.2985E+02	.1708E+03
18	.2985E+02	.1708E+03

Normal contact stiffness (rock/fence) = .1944E+06
Maximum fence penetration = .5000E+00

Normal contact stiffness (fence/fence) = .2522E+06
Maximum fence penetration = .5000E+00

Normal contact stiffness (ground/rock) = .8723E+08
Information: S/R chekdt - time step = .827E-04
note, max. stable time step = .827E-04

max time step governed by axial stiffnesses
of element no. = 3

time = .496E-02 secs

el.	x	y	theta	vx	vy	ang-v
1	.000E+00	-.500E+01	.000E+00	.000E+00	.000E+00	.000E+00
2	.216E+01	-.402E-03	.165E+00	-.490E+02	-.158E+00	.306E+02
3	-.428E-01	.166E-05	.591E-03	-.200E+02	.179E-02	.378E+00
4	-.228E-04	.545E-01	.266E-04	-.204E-01	-.215E-02	.237E-01
5	-.429E-07	.218E+00	.500E-07	-.517E-04	-.148E-05	.603E-04
6	-.474E-10	.490E+00	.552E-10	-.725E-07	-.149E-08	.845E-07
7	-.336E-13	.871E+00	.392E-13	-.627E-10	-.201E-11	.730E-10
8	-.165E-16	.136E+01	.192E-16	-.361E-13	.148E-12	.421E-13
9	-.585E-20	.196E+01	.682E-20	-.147E-16	-.280E-12	.172E-16
10	.000E+00	.550E+01	.000E+00	.000E+00	.000E+00	.000E+00
11	-.260E+01	.384E-17	.000E+00	.000E+00	.152E-14	.000E+00

12	-.260E+01	.545E-01	.000E+00	.000E+00	.182E-15	.000E+00
13	-.260E+01	.218E+00	.000E+00	.000E+00	-.109E-14	.000E+00
14	-.260E+01	.490E+00	.000E+00	.000E+00	.200E-15	.000E+00
15	-.260E+01	.871E+00	.000E+00	.000E+00	-.101E-14	.000E+00
16	-.260E+01	.136E+01	.000E+00	.000E+00	.148E-12	.000E+00
17	-.260E+01	.196E+01	.000E+00	.000E+00	-.280E-12	.000E+00
18	-.260E+01	.550E+01	.000E+00	.000E+00	.000E+00	.000E+00

time = .993E-02 secs

el.	x	y	theta	vx	vy	ang-v
1	.000E+00	-.500E+01	.000E+00	.000E+00	.000E+00	.000E+00
2	.196E+01	-.154E-02	.310E+00	-.332E+02	-.295E+00	.285E+02
3	-.194E+00	.262E-03	.160E-02	-.377E+02	.224E+00	-.945E+00
4	-.791E-03	.543E-01	.922E-03	-.454E+00	-.988E-01	.529E+00
5	-.430E-05	.218E+00	.501E-05	-.303E-02	-.461E-03	.354E-02
6	-.156E-07	.490E+00	.182E-07	-.134E-04	-.167E-05	.156E-04
7	-.393E-10	.871E+00	.458E-10	-.400E-07	-.799E-08	.466E-07
8	-.711E-13	.136E+01	.829E-13	-.843E-10	-.449E-10	.982E-10
9	-.962E-16	.196E+01	.112E-15	-.130E-12	-.778E-12	.152E-12
10	.000E+00	.550E+01	.000E+00	.000E+00	.000E+00	.000E+00
11	-.260E+01	-.123E-04	.139E-03	-.110E+01	-.557E-01	.537E+00
12	-.260E+01	.545E-01	.562E-08	-.353E-04	-.858E-06	.411E-04
13	-.260E+01	.218E+00	.679E-13	-.547E-09	-.140E-10	.638E-09
14	-.260E+01	.490E+00	.332E-18	-.312E-14	.379E-15	.363E-14
15	-.260E+01	.871E+00	.000E+00	.000E+00	-.202E-14	.000E+00
16	-.260E+01	.136E+01	.000E+00	.000E+00	.296E-12	.000E+00
17	-.260E+01	.196E+01	.000E+00	.000E+00	-.561E-12	.000E+00
18	-.260E+01	.550E+01	.000E+00	.000E+00	.000E+00	.000E+00

time = .149E-01 secs

el.	x	y	theta	vx	vy	ang-v
1	.000E+00	-.500E+01	.000E+00	.000E+00	.000E+00	.000E+00
2	.183E+01	-.342E-02	.444E+00	-.211E+02	-.477E+00	.252E+02
3	-.357E+00	.769E-03	-.800E-02	-.307E+02	-.770E+00	-.344E+01
4	-.725E-02	.530E-01	.845E-02	-.225E+01	-.405E+00	.262E+01
5	-.940E-04	.218E+00	.110E-03	-.494E-01	-.248E-01	.576E-01
6	-.638E-06	.490E+00	.744E-06	-.399E-03	-.153E-03	.465E-03
7	-.314E-08	.871E+00	.366E-08	-.229E-05	-.133E-05	.267E-05
8	-.116E-10	.136E+01	.135E-10	-.971E-08	-.149E-07	.113E-07
9	-.331E-13	.196E+01	.385E-13	-.313E-10	-.198E-09	.365E-10
10	.000E+00	.550E+01	.000E+00	.000E+00	.000E+00	.000E+00
11	-.266E+01	.193E-02	-.599E-03	-.194E+02	.163E+01	-.242E+00
12	-.260E+01	.545E-01	.630E-04	-.363E-01	-.414E-02	.423E-01
13	-.260E+01	.218E+00	.184E-06	-.157E-03	-.769E-05	.183E-03
14	-.260E+01	.490E+00	.281E-09	-.321E-06	-.163E-07	.374E-06
15	-.260E+01	.871E+00	.260E-12	-.370E-09	-.397E-10	.431E-09
16	-.260E+01	.136E+01	.160E-15	-.272E-12	.357E-12	.317E-12
17	-.260E+01	.196E+01	.408E-19	-.109E-15	-.841E-12	.126E-15
18	-.260E+01	.550E+01	.000E+00	.000E+00	.000E+00	.000E+00

II.5.3 Sample Geometry Plotting Session

The following output is from the computer screen during a sample session using GPLOT, the interactive geometry plotting module. This session produces an animation of the sample2 analysis:

NOTES:
(i) The command g executes a batch file g.bat which executes gplot from a subdirectory.
(ii) The user responses are prefixed with >.

```
>g
Enter input-data file name (Exclude Ext.) : sample2
 Enter Plotting Time:
>11
 do you want to plot element numbers (y/n)?
>n
 current window coordinates are:
 x-min    y-min    x-max    y-max
 -10.0    -15.0     10.0     9.69
 do you want to change the window coords (y/n)?
>n
 animate or single frame (a/s) ?
>a

Stop - Program terminated.
```

The hardcopy output from grock.ps is shown in Figure II.5 below.

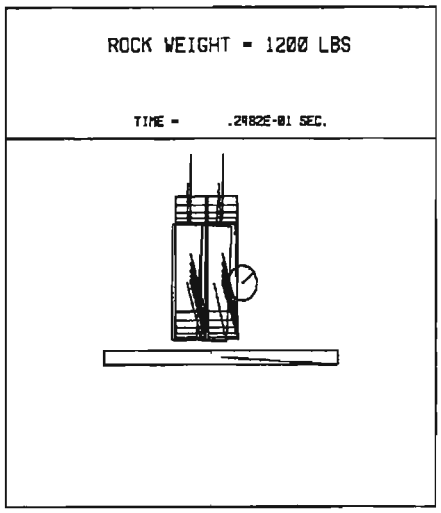

Figure II.5 A Geometry Snapshot Plot

II.5.4 Sample Time History Plotting Session

The following output is from the computer screen during a sample session using HPLOT the interactive time history plotting module. This session produces a time history of the x-component of the rock velocity throughout the impact for the sample2 analysis. A hardcopy file called vrock.ps is created during the session. The hardcopy output from vrock.ps is shown in Figure II.6:

NOTE: The command h executes a batch file h.bat which executes hplot from a subdirectory.

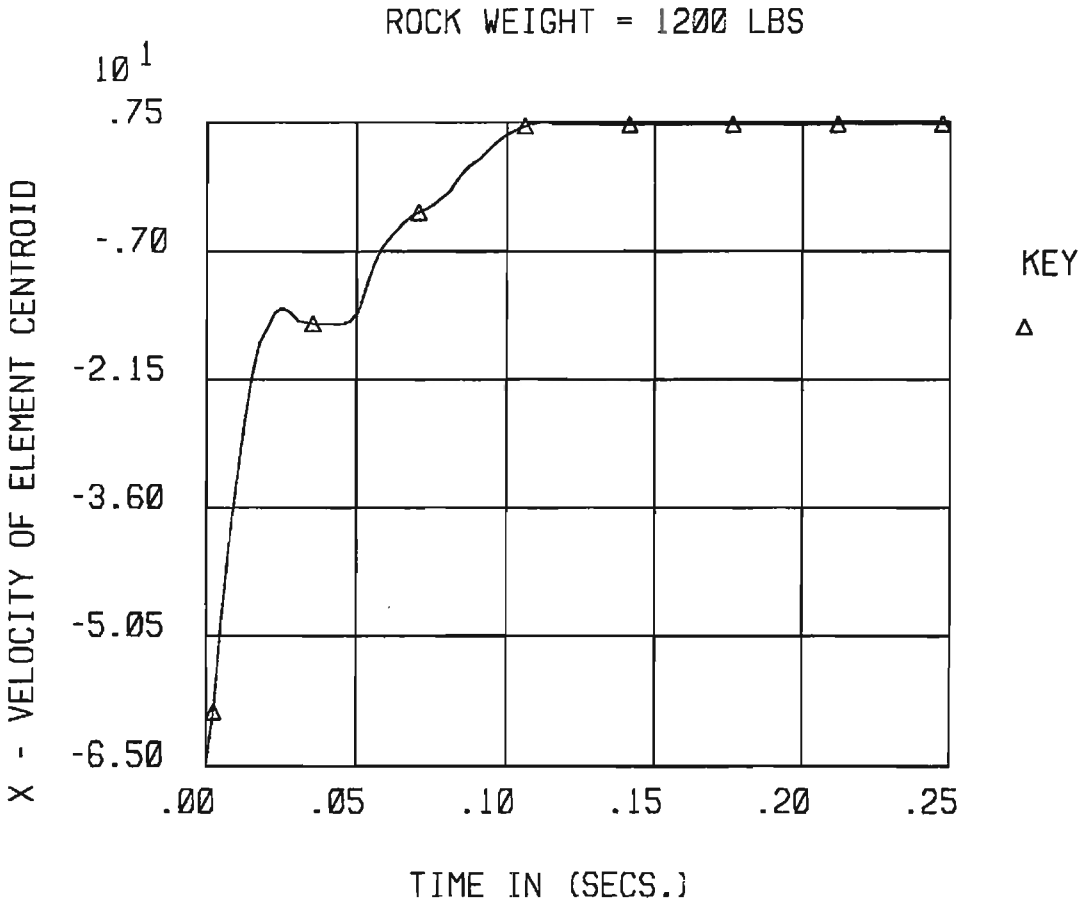

Figure II.6 Time History of x-component of Rock Velocity

```
C:\GRAHAM\FENCE>h

C:\GRAHAM\FENCE>hplot\hist
 ENTER HISTORY PLOT FILENAME (20 CHARACTERS MAX.)
sample2
 Select from Available Elements Numbers:
  2   3   4   5   6
Enter Element Number:
2
 Element Number  2 is Selected
Do you want to select another element?
Enter y(es) or n(o)
n
 Select y-values from available components:
 Case:   1 FORCE IN TOP JOINT OF ATTENUATOR
 Case:   2 TENSION IN BOTTOM CABLE
 Case:   3 TENSION IN TOP CABLE
 Case:   4  X - VELOCITY OF ELEMENT CENTROID
 Case:   5  Y - VELOCITY OF ELEMENT CENTROID
 Case:   6 ANGULAR VELOCITY OF ELEMENT - OMEGA
 Case:   7 ELEMENT KINETIC ENERGY (TRANSLATIONAL)
 Case:   8 ELEMENT KINETIC ENERGY (ROTATIONAL)
Enter Case Number:
4




 Case:   7 ELEMENT KINETIC ENERGY (TRANSLATIONAL)
 Case:   8 ELEMENT KINETIC ENERGY (ROTATIONAL)
Enter Case Number:
4
 X - VELOCITY OF ELEMENT CENTROID          is Selected
Do you want to plot element x-values
n
 Enter Plotting Time:
11
do you want to change plotting titles ?
 ROCK WEIGHT = 1200 LBS

n
do you want to change plotting x-title ?
TIME IN (SECS.)
n
do you want to change plotting y-title ?
 X - VELOCITY OF ELEMENT CENTROID
n
do you want to change ymin, ymax ?
ymin =    -.6500E+02 ymax =     .7456E+01
n
do you want to change no. of x and y grid divisions ?
ndivx =    5 ndivy =    5
n
```


```
Do you want a hardcopy output file (y/n)?
y
 enter filename - max 20 characters
vrock.ps
Hardcopy file is vrock.ps

do you want to dump history data to a file (y/n) ?
y
 enter data file name, 40 characters max.
vrock
 data file name is:
vrock.RAW
 enter return to continue


Do you want to do another plot,new plot file or quit?
Enter a(nother)/n(ew)/q(uit)
```

```
Stop - Program terminated.
```